Morphology, structure and evolution of California Continental Borderland restraining bends

Article *in* Geological Society London Special Publications · January 2007

DOI: 10.1144/SP290.3

5 authors, including:

Mark R. Legg
Legg Geophysical, Inc.
55 PUBLICATIONS **529** CITATIONS
SEE PROFILE

Chris Goldfinger
Oregon State University
278 PUBLICATIONS **2,731** CITATIONS
SEE PROFILE

Morphology, structure and evolution of California Continental Borderland restraining bends

M.R. Legg, C. Goldfinger, M. J. Kamerling, J. D. Chaytor and D. E. Einstein

Geological Society, London, Special Publications 2007; v. 290; p. 143-168
doi:10.1144/SP290.3

Morphology, structure and evolution of California Continental Borderland restraining bends

M. R. LEGG[1], C. GOLDFINGER[2], M. J. KAMERLING[3], J. D. CHAYTOR[2] & D. E. EINSTEIN[4]

[1]*Legg Geophysical, Huntington Beach, CA 92647, USA (e-mail: mrlegg@attglobal.net)*

[2]*College of Oceanic and Atmospheric Sciences, Oregon State University, Corvallis, OR 97331, USA*

[3]*Venoco, Inc., Carpinteria, CA 93013, USA*

[4]*Southern California Earthquake Center, Los Angeles, CA 90089, USA*

Abstract: Exceptional examples of restraining and releasing bend structures along major strike-slip fault zones are found in the California continental Borderland. Erosion in the deep sea is diminished, thereby preserving the morphology of active oblique fault deformation. Long-lived deposition of turbidites and other marine sediments preserve a high-resolution geological record of fault zone deformation and regional tectonic evolution. Two large restraining bends with varied structural styles are compared to derive a typical morphology of Borderland restraining bends. A 60-km-long, 15° left bend in the dextral San Clemente Fault creates two primary deformation zones. The southeastern uplift involves 'soft' turbidite sediments and is expressed as a broad asymmetrical ridge with right-stepping en echelon anticlines and local pull-apart basins at minor releasing stepovers along the fault. The northwest uplift involves more rigid sedimentary and possibly igneous or metamorphic basement rocks creating a steep-sided, narrow and more symmetrical pop-up. The restraining bend terminates in a releasing stepover basin at the NW end, but curves gently into a transtensional releasing bend to the SE. Seismic stratigraphy indicates that the uplift and transpression along this bend occurred within Quaternary times. The 80-km-long, 30–40° left bend in the San Diego Trough–Catalina fault zone creates a large pop-up structure that emerges to form Santa Catalina Island. This ridge of igneous and metamorphic basement rocks has steep flanks and a classic 'rhomboid' shape. For both major restraining bends, and most others in the Borderland, the uplift is asymmetrical, with the principal displacement zone lying along one flank of the pop-up. Faults within the pop-up structure are very steep dipping and subvertical for the principal displacement zone. In most cases, a Miocene basin has been structurally inverted by the transpression. Development of major restraining bends offshore of southern California appears to result from reactivation of major transform faults associated with Mid-Miocene oblique rifting during the evolution of the Pacific–North America plate boundary. Seismicity offshore of southern California demonstrates that deformation along these major strike-slip fault systems continues today.

Restraining bends are present along strike-slip faults where fault curvature or offset en échelon fault segments tend to impede smooth lateral motion of opposing crustal blocks (Crowell 1974). On right-lateral faults, as along the Pacific–North America transform plate boundary, a restraining bend exists where the fault curves or steps to the left when following the fault trace. Crowding of crustal material by lateral movement into the fault bend produces uplift and crustal thickening by folding and thrust or reverse faulting adjacent to the principal displacement zone (PDZ) of the active strike-slip fault. Such zones are called transpressional (Harland 1971) or convergent strike-slip fault zones (Biddle & Christie-Blick 1985; Sylvester 1988). In contrast, releasing bends or transtensional zones exist where the fault bends or steps to the right for dextral systems. Large-scale transtension results in crustal thinning and basin formation by normal faulting and subsidence adjacent to the PDZ. In the simple fault bend model, deformation is expected to concentrate adjacent to the maximum fault curvature (Fig. 1). This paper examines the morphology and shallow-crustal structure of restraining bends along active strike-slip faults in the southern California region, with a focus on the offshore area, i.e. the California Continental Borderland. From comparison of analogue models of restraining bend geometry and progressive evolution to well-defined Borderland examples,

From: CUNNINGHAM, W. D. & MANN, P. (eds) *Tectonics of Strike-Slip Restraining and Releasing Bends.* Geological Society, London, Special Publications, **290**, 143–168.
DOI: 10.1144/SP290.3 0305-8719/07/$15.00

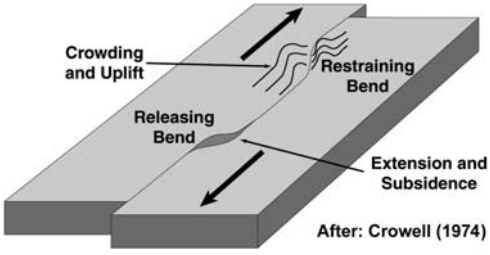

Fig. 1. Material crowded into a restraining bend along a strike-slip fault results in convergence, folding and reverse faulting that creates a local uplift. In contrast, extension and subsidence occurs at a releasing bend.

a better understanding of the structural development and tectonic evolution of restraining bends is derived.

Restraining bend geometry is mechanically unfavourable for strike-slip faulting (Segall & Pollard 1980). In homogeneous media, fault linkages between en échelon and discontinuous fault segments are more likely to form within a releasing geometry, where local extension favours crack growth and propagation. Nevertheless, irregular fault geometry produces abundant restraining bends along strike-slip faults. Bends range in scale from localized jogs in earthquake surface ruptures to crustal-scale uplifts with surface deformation exceeding lengths of 100 km along the fault (Crowell 1974; Sylvester & Smith 1976; Mann *et al.* 1985; Anderson 1990; Butler *et al.* 1998). Consequently, special crustal conditions must be involved to form restraining bends. Possible conditions include pre-existing structural fabric and other crustal heterogeneity, and changing strain fields and related stress fields that alter deformation styles on existing fault systems or create new faults to accommodate the evolving strain field (cf. Dewey *et al.* 1998). Careful studies of well-defined fault bends are needed to deduce the processes involved in restraining-bend formation and evolution.

Finite deformation within long-lived restraining bends results in pronounced topographic expression, called push-up or 'pop-up' structures (cf. Stone 1995; Dewey *et al.* 1998; McClay & Bonora 2001). In contrast, releasing bends create basins, which become filled with sediments that tend to smooth and obscure their morphology. Deformation along oblique strike-slip fault segments tends to occur over broad zones (Wilcox *et al.* 1973; Schreurs & Colletta 1998; Withjack & Jamison 1986; McClay & Bonora 2001), commonly many kilometres wide. The pop-up morphology, even though modified by erosion or other destructive processes, can provide a direct measure of the accumulated deformation along the restraining bend (cf. Wakabayashi 2007). Basin-filling sedimentary sequences record the history of deformation along both restraining and releasing fault bends. Quantification of the bend evolution and inference of the larger-scale processes along the more regional strike-slip fault system are possible using geophysical techniques, like seismic reflection profiling, to measure and map the deformation.

Large restraining bends in active strike-slip faults impede crustal block motion, locally enhancing the accumulation of tectonic stresses that may produce major earthquakes, e.g. 1857 Fort Tejon, California (Sieh 1978); 1989 Loma Prieta, California (Plafker & Galloway 1989; Schwartz *et al.* 1994); and 1999 Izmit and Duzce, Turkey (Aydin & Kalafat 2002; Harris *et al.* 2002). Detailed investigations of mainshock and aftershock sequences for restraining-bend earthquakes provide important data regarding the deeper crustal structure (Seeber & Armbruster 1995). However, if restraining bends are locked between large earthquakes, seismicity in the bend area may be low, and other geophysical methods must be used to evaluate deep bend structure (cf. Langenheim *et al.* 2005).

Many bend structures are buried under thick sedimentary blankets, as in the Los Angeles basin (Fig. 2), and changing tectonic conditions associated with an evolving plate boundary tend to obscure the processes directly related to the restraining bend evolution. The uplift, folding and faulting associated with large restraining bends often form excellent traps for hydrocarbons. Numerous productive oil fields, especially in southern California (Harding 1973, 1974; Wright 1991), exist along active strike-slip faults and are associated with restraining bends. Subsurface samples from wells and boreholes provide stratigraphic control that supplements geophysical data for interpretation of the structural geometry and deformation history of restraining bends.

California Continental Borderland

The California Continental Borderland (Fig. 2) is a mostly submerged part of the Pacific–North America dextral transform plate boundary that exhibits a basin-and-ridge physiography (Shepard & Emery 1941; Moore 1969). Right-slip on irregular fault traces has produced numerous restraining bend pop-ups that exhibit distinctive seafloor morphology. The submarine basins of the Borderland range in depth from a few hundred metres to more than 2000 m and are variably filled with clastic sediments from the adjacent mainland and offshore islands. Erosion is greatly diminished in these deep basins compared with subaerial regions, so that pop-up morphology is well preserved on the

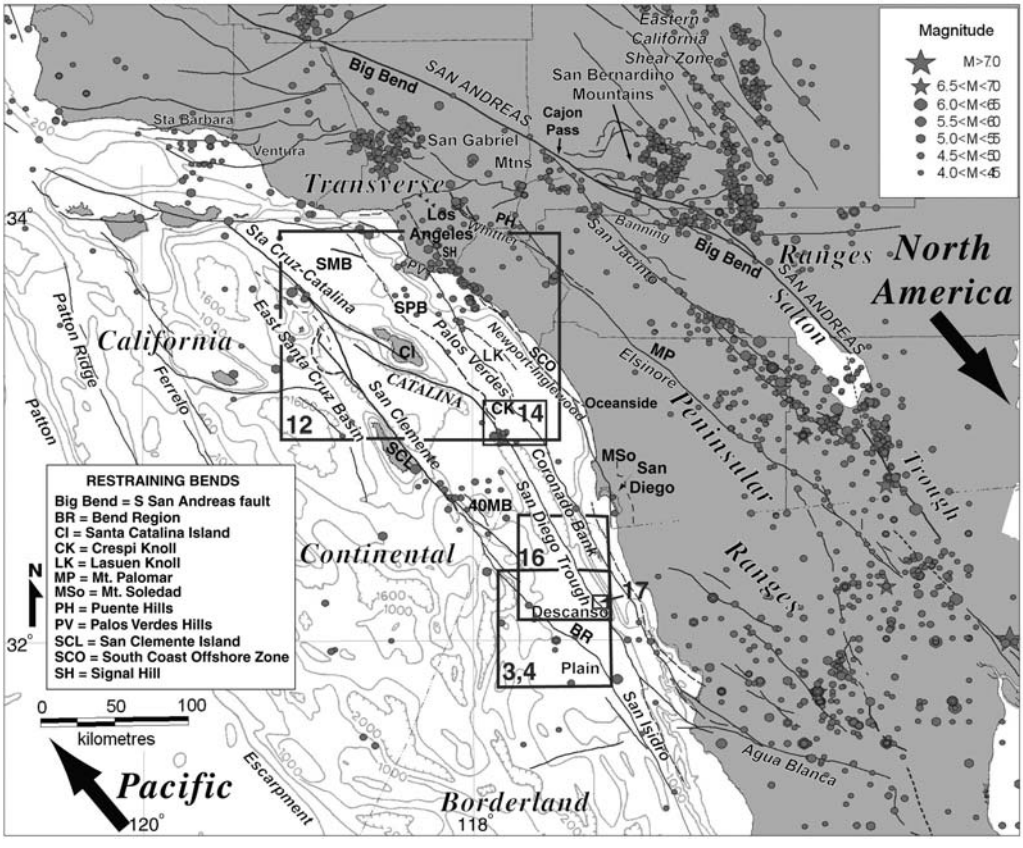

Fig. 2. Location map of seismicity in southern California region and major physiographic provinces. Major fault zones are labelled at some of the more significant restraining bends in the region. Large arrows indicate relative plate-motion vectors for transform faulting between the Pacific and North American plates. Contours in the offshore area are in metres. Rectangles labelled with figure numbers outline locations of detailed maps. SMB, Santa Monica Basin, SPB, San Pedro Basin; 40MB, Fortymile Bank.

seafloor. Deformation history is recorded in well-bedded turbidite and other sedimentary sequences that fill these submarine basins. Using multi-beam bathymetry and seismic reflection profiling, several prominent restraining bend pop-ups within the Borderland are examined, with a focus on two large structural culminations: the San Clemente Fault bend region and the Santa Catalina Island uplift. From our observations, the typical morphology of Borderland restraining bends is described, followed by presentation of a model for the initiation and geological evolution of Borderland restraining bends.

Specific examples of restraining bend pop-ups located within the California Continental Borderland are described and compared with the general model. Where data allow, the age of the bend uplift is estimated and the history of deformation is inferred. These interpretations lead to several conclusions regarding the formation and development of restraining bends along the California continental margin and the Pacific–North America transform plate boundary.

Data

High-resolution contour and shaded relief maps created from processed multi-beam swath bathymetry (Fig. 3) and, where necessary, older single-beam echo-sounder records provide excellent images of the seafloor morphology of strike-slip fault bend structures (NOS 1999; Goldfinger *et al.* 2000; K. Macdonald 2003, pers. comm.). Lateral resolution of mapped features is about 50 to 100 m for areas of multibeam coverage in this study where water depths exceed 1000 m. Areas mapped using single-beam soundings have somewhat lower spatial resolution, mostly within about

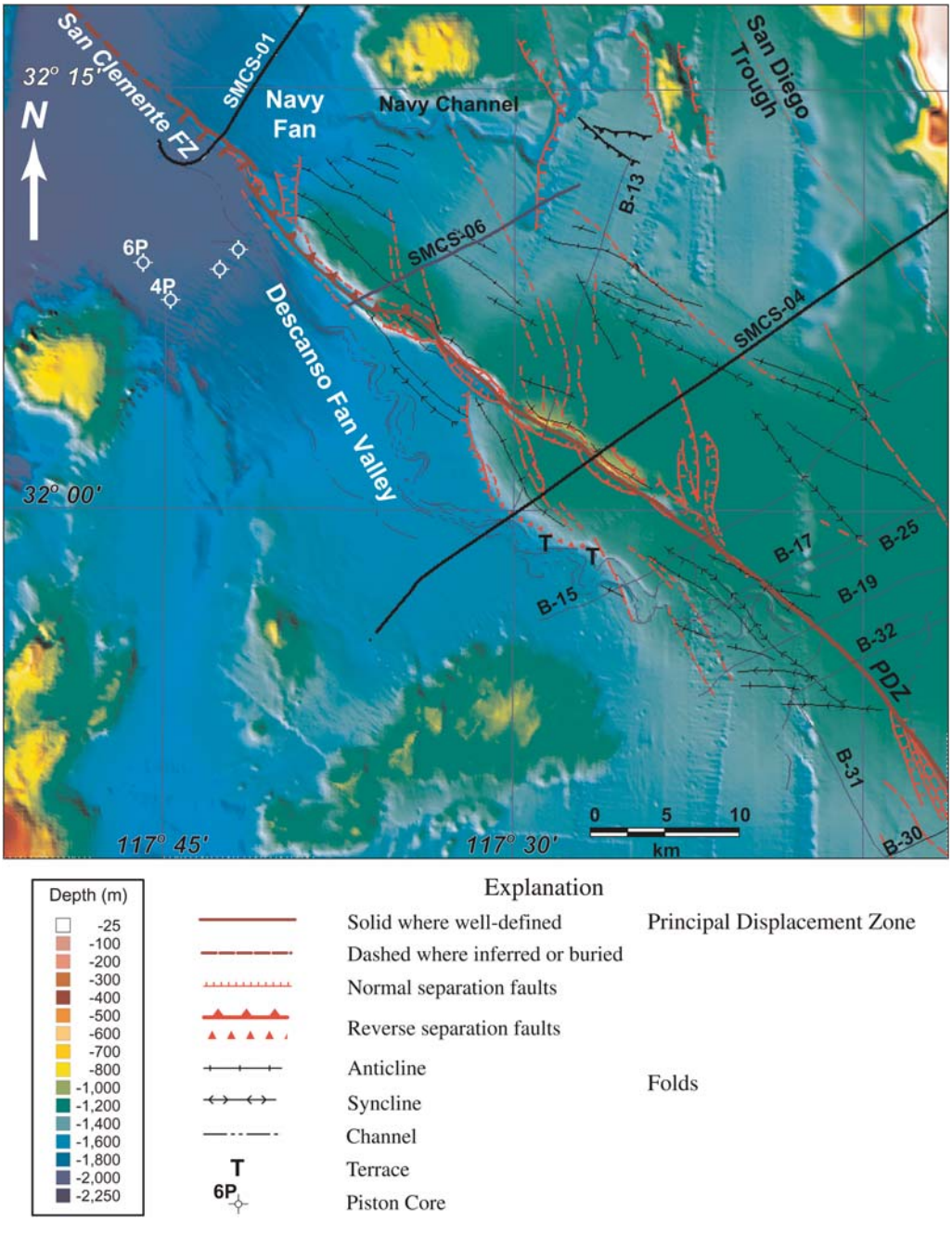

Fig. 3. Map of geological structures along the bend region of the San Clemente Fault (see Fig. 2 for map location). Bathymetry is a compilation of multi-beam and older echo-soundings. Two distinct uplifts, one cored by bedrock, the other in turbidite sediments, comprise the pop-up structure. The principal displacement zone (PDZ) cuts a relatively straight path through the restraining bend, with a gentle curve at the SE end and a right-stepover at the NW end. Branch and secondary faults within the pop-up are generally reverse separation, probably oblique-slip, and trend north to NW, subparallel to the PDZ. Folds are also subparallel to the PDZ within the bend, but trend east–west beyond the transpressional section at the SE end.

500 m. Vertical resolution decreases with increasing depth, but is usually within 2% of the water depth for absolute depth, about 20 to 40 m for the Borderland basins, and within about 5 to 10 m for relative depths within a basin. Oblique three-dimensional shaded relief views (such as Fig. 4) emphasize the seafloor uplift and tectonic geomorphology associated with strike-slip faults and restraining and releasing bends.

High-resolution analogue seismic-reflection profiles acquired using airgun, sparker and 3.5 kHz transducer sources (Vedder *et al.* 1974; Legg 1985) are used to interpret the sub-seafloor character of the faults and prominent stratigraphic sequences associated with the major submarine fans of the Borderland (Figs 5–6). Although the analogue profiles are unmigrated, the dip of shallow reflecting horizons is shallow ($<5^{\circ}$), and steep faults are recognized by reflector terminations or diffractions (cf. Tucker & Yorston 1973). Structural contours and isopachs of shallow sedimentary sequences were mapped based on the seismic interpretations. Sequence ages were estimated based on sedimentation rates derived from shallow piston cores in the Borderland basins (Emery 1960; Heath *et al.* 1976; Dunbar 1981; Legg 1985), and used to infer the deformation history along the fault bends. Additional stratigraphic control was provided from outcrop samples, dart cores, and borehole data where older sedimentary, volcanic and metamorphic bedrock is exposed in the pop-up (Vedder *et al.* 1974; Vedder 1990).

Digitally recorded, high-resolution, multichannel seismic profiles (MCS) across major segments of the fault bends are used to image the deeper fault structure and sediment deformation, and to measure fault dips and offsets (Figs 7–8; Bohannon *et al.* 1990, K. Macdonald, 2003, pers. comm.). Navigation for these recent seismic surveys was provided by GPS, and geographical positional accuracy within about 10 m is estimated. Conventional two-dimensional seismic data-processing schemes were used for the MCS profiles to prepare common mid-point stack and frequency-wavenumber migrated images. Seismic

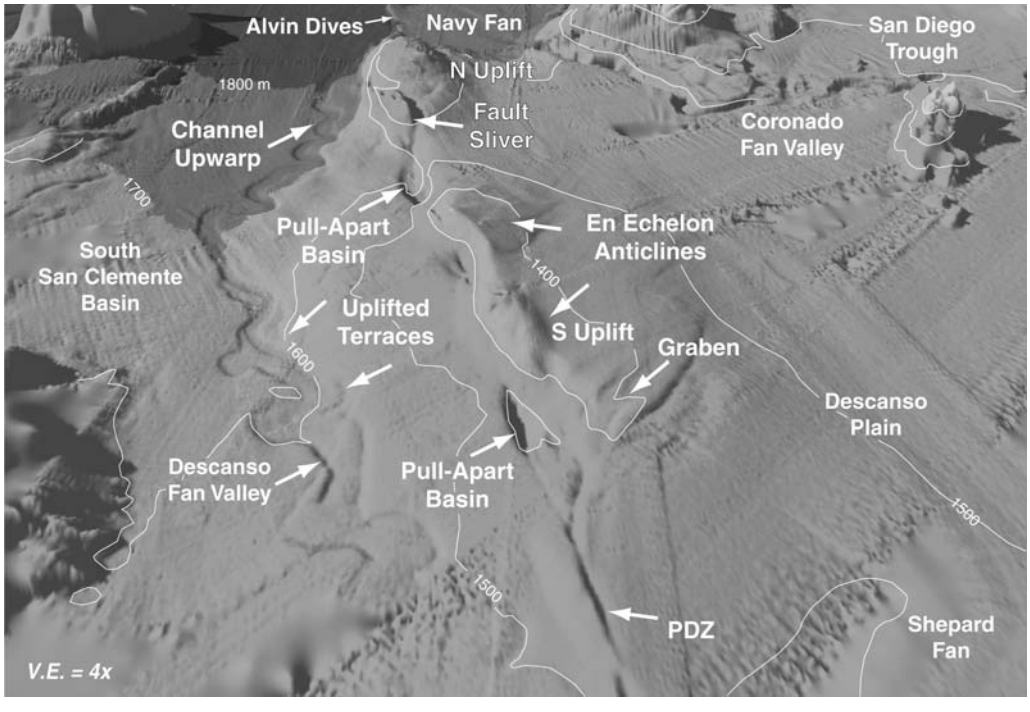

Fig. 4. Perspective shaded-relief view looking NW along the bend region of the San Clemente Fault. The principal displacement zone cuts across the image from bottom right centre to upper left centre. Prominent tectonic geomorphic features are identified that indicate right-slip fault character and seafloor uplift due to oblique convergence along the restraining bend. The bedrock uplift in the NW is steep-sided and more symmetrical than the broad asymmetrical SE uplift in the turbidites. Bathymetric contour values are in metres; the distance along fault is about 60 km from bottom to top.

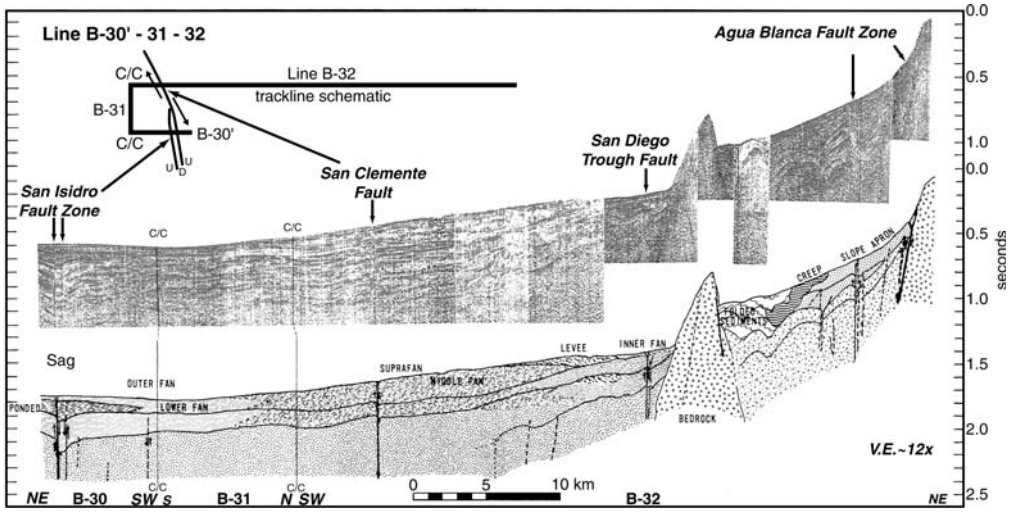

Fig. 5. Sparker seismic profile (line B-30[1]–31-32; see Fig. 3 for profile location) across the Descanso Plain, showing the character of well-defined strike-slip faults away from restraining bends. Two course changes between lines are indicated (C/C). San Clemente Fault is straight and narrow with a strike parallel to the relative plate-motion vector (320°). San Isidro Fault zone is a releasing fault bend, striking about 330°, creating a transtensional sag or stepover basin evident between en échelon fault traces. The San Isidro fault zone represents the southern continuation of the San Clemente fault zone west of Baja California. San Diego Trough Fault is also a straight and narrow right-slip fault across this profile; minor transpression is evident at depth for the Agua Blanca fault zone.

velocities used for migration are based on stacking velocities, seismic refraction and wide-angle reflection profiling in the area (Moore 1969; Shor *et al.* 1976).

Borderland restraining bend morphology

A generalized model of the restraining bend pop-up morphology (Fig. 9) is derived from interpretations of data along the San Clemente Fault bend region in the Descanso Plain offshore of NW Baja California (Figs 2–4). This model represents a double bend, where the fault bends first to the left and then bends back to the original strike. A transpressional zone forms within the restraining double bend and is manifest as a prominent seafloor uplift that may be a complex structure consisting of right-stepping en echelon anticlines with intervening subsidiary extensional strike-slip basins and diverging oblique-slip fault zones (Figs 3–4). The uplift is broadly asymmetrical, with the principal displacement zone (PDZ) of the active strike-slip fault located to one side of the axis of uplift. Typically, the PDZ is vertical for well-defined strike-slip faults in the bend. Reverse faults that probably accommodate oblique-slip exist along the flanks of the uplift and trend subparallel to the PDZ. Beyond the ends of the restraining double bend, oblique extension forms strike-slip basins that may occur as pull-apart (stepover) or sag (releasing bend) basins.

North-northwest trending dip-slip (oblique-slip?) faults that diverge from the PDZ could be interpreted as antithetic Riedel shears (Fig. 9), but their observed trend is about midway between that predicted for synthetic and antithetic faults (e.g. Wilcox *et al.* 1973). Instead, they trend subparallel to the predicted trend for extension fractures. Although superficially these appear to form grabens bounded by normal faults (Fig. 4), based on seismic profiles they are upthrusts with reverse separation (Fig. 7, SMCS04, shot 4250). According to Billings (1972, p. 198), an upthrust is a high-angle fault 'along which the relatively uplifted block has been the active element.' The upthrusts elevate the pop-up and create grabens in places where local uplift lags that of adjacent blocks. Some reverse faults in Borderland restraining bends trend east–west as predicted from the wrench fault model, but most trend subparallel to the PDZ. This indicates strain partitioning, with reverse faults accommodating shortening and vertical faults accommodating strike-slip.

North- to NW-trending normal-separation (oblique-normal?) faults also exist in the sediments above an acoustic basement block to the west of the PDZ (Figs 3 & 7); these result from stretching of the

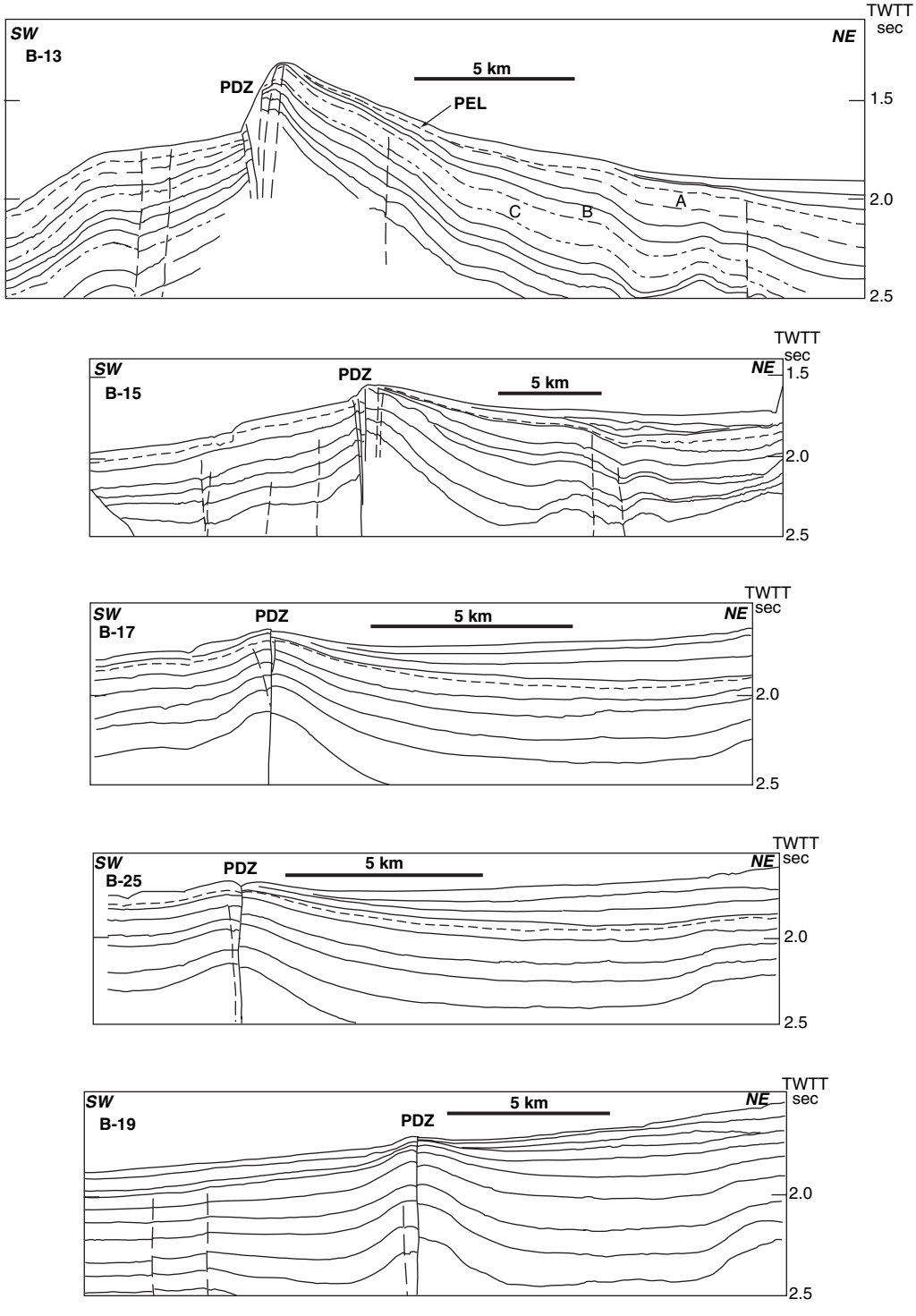

Fig. 6. Line drawings of sparker seismic profiles (see Fig. 3 for profile locations) across the restraining bend region of the San Clemente Fault show a broad zone of faulting and uplift due to transpression, compared with simple parallel right-slip (cf. Fig. 5). Significant stratigraphic horizons are shown to indicate the increasing deformation with depth and time. Uplift rates for the pop-up structure are derived from horizons PEL, A, B and C. The sequence stratigraphic unit PEL is a Late Quaternary hemipelagic layer based on acoustic transparency (Figs 7 & 11).

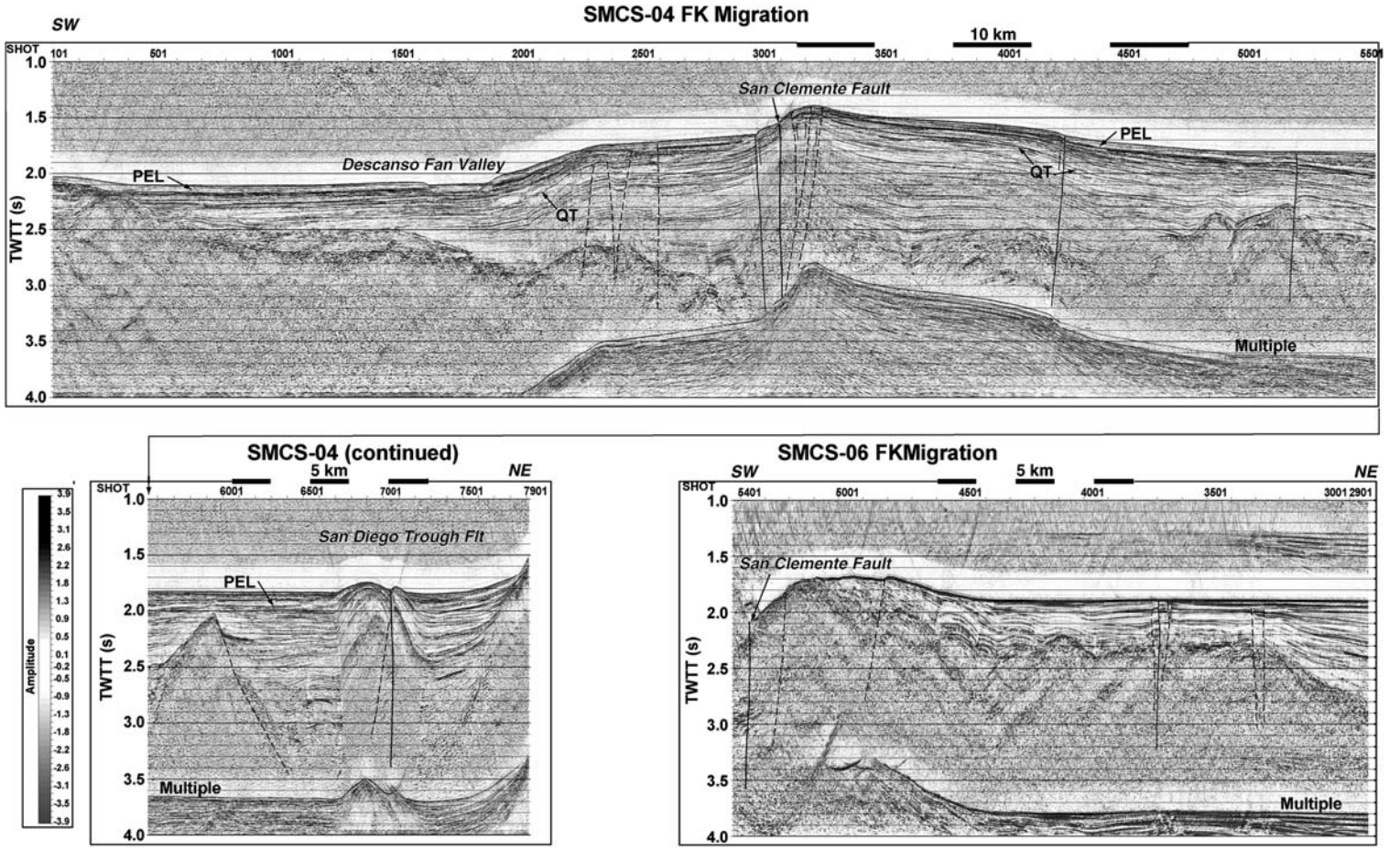

Fig. 7. High-resolution MCS profiles across the bend region of the San Clemente Fault (see Fig. 3 for profile locations) showing the broad zone of deformation in the pop-up structure. Data are post-stack migrated, 12-fold with 1.56 m CMP trace spacing. The principal displacement zones for the San Clemente and San Diego Trough faults are bold solid lines; other faults are solid where well-defined, and dashed where buried or less well-defined. Late Quaternary sequence PEL is hemipelagic based on its acoustic transparency. Some thin turbidite sand layers are found in this unit, based on piston-core samples from the nearby San Clemente basin and Navy fan (Dunbar 1981). Horizon QT represents the top of the pre-uplift turbidite sediments, and records the beginning of transpression.

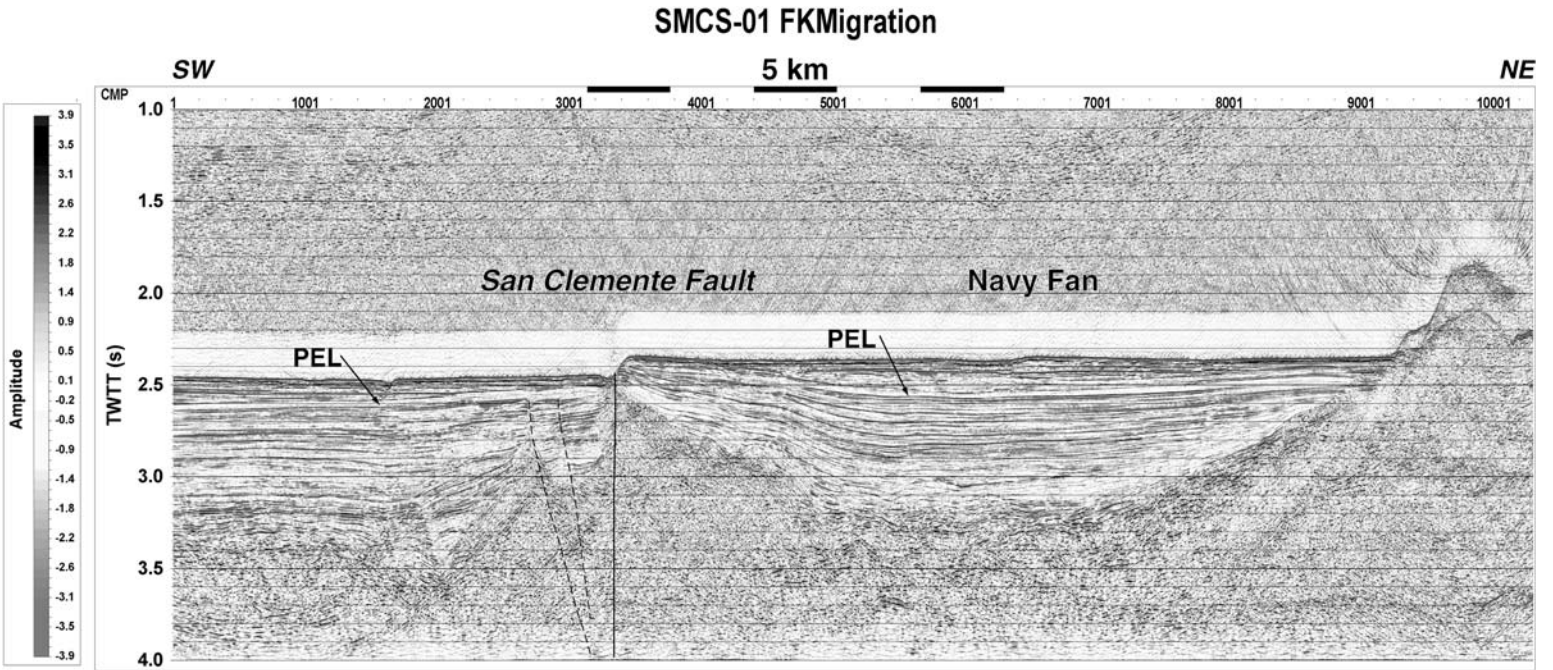

Fig. 8. High-resolution MCS profile across the north end of the San Clemente Fault bend region (see Fig. 3 for profile location). Data processing is the same as for Figure 7. DSV Alvin submersible dives observed vertical seafloor scarps, 1 to 3 m high in mud on the 100-m-high San Clemente Fault escarpment near this profile (Fig. 10). Hemipelagic unit PEL is buried beneath young turbidites of the Navy Fan, but may crop out in the escarpment.

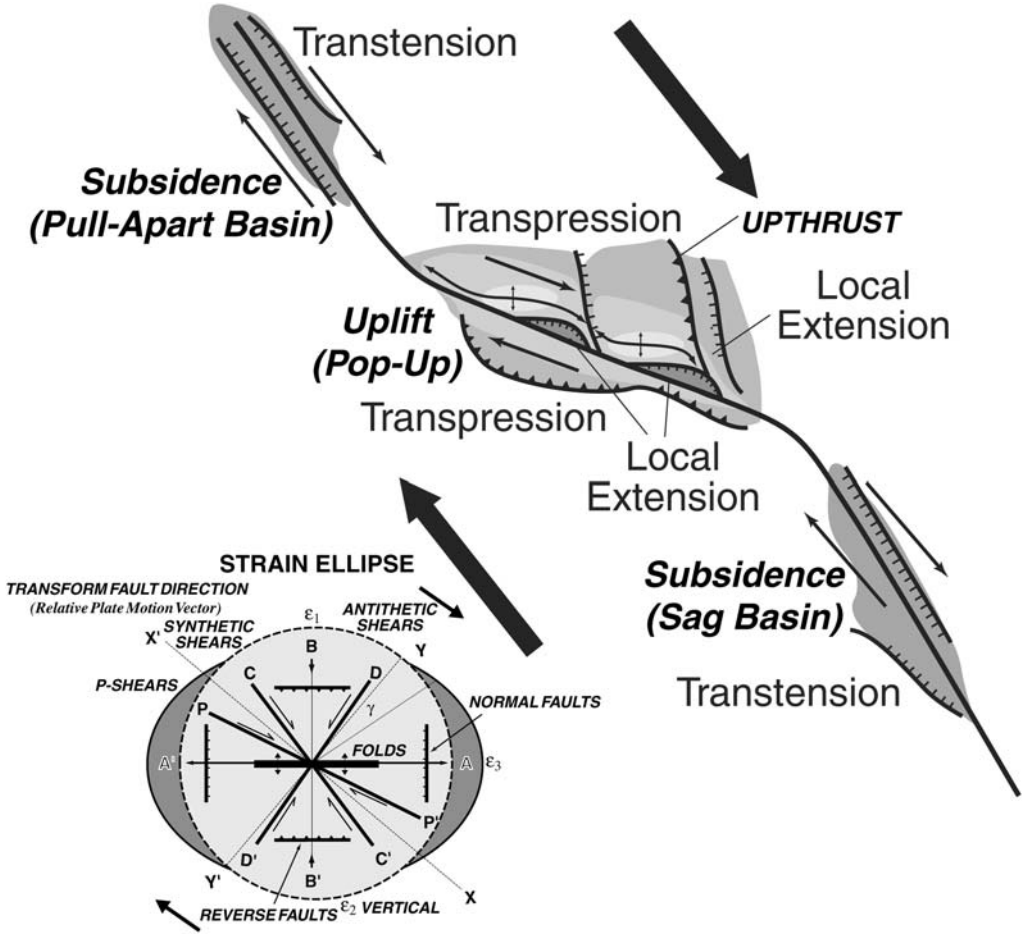

Fig. 9. Typical morphology and structure of restraining double bends in southern California, based on the San Clemente Fault bend region. Some features may be missing on other restraining bends, but some features may be more pronounced than in the San Clemente Fault example. Most Borderland restraining double bends have transtensional zones at the ends. A strain ellipse is shown to highlight the expected structural character for different trends in a zone of NW-directed dextral shear (after Wilcox *et al.* 1973). Contrary to the expected strain patterns, the north-trending faults in the San Clemente Fault bend region are steeply dipping upthrusts, not normal faults.

sedimentary cover as the basement pushes upward due to overall transpression. In other areas, such as the Palos Verdes Hills (Fig. 2), shallow 'keystone' grabens form by extension along the crest of the transpressional uplift (Woodring *et al.* 1946; Francis *et al.* 1999).

In contrast, northwest-trending faults that bound the extensional basins beyond the ends of the restraining double bend are subparallel to the PDZ and commonly exist along monoclinal sags that dip inward to the PDZ (Fig. 5, San Isidro fault zone). This also indicates strain partitioning between normal (oblique?) faults on the flanks of the PDZ that accommodate extension, and a vertical PDZ that accommodates strike-slip. Most faults observed in seismic profiles across Borderland restraining bends have steep dips, measured at 70 to 80° for secondary oblique-slip(?) faults and vertical for the PDZ.

San Clemente Fault bend region

The San Clemente fault zone, with an overall length exceeding 600 km, is an active member of the larger San Andreas fault system that defines the dextral Pacific–North America (PAC–NOAM) transform plate boundary (Fig. 2; Legg 1985; Legg *et al.* 1989). The average strike of the San Clemente

Fault is about 320° (Figs 2–3), parallel to Recent PAC–NOAM relative motion (Minster & Jordan 1978; Demets *et al.* 1990). Segments of the San Clemente Fault that strike 320° are simple, narrow and well-defined in character (Fig. 5, San Isidro Fault), consistent with 'parallel strike-slip' (Legg 1985). Fault segments that bend to the right or are more north-trending are extensional (transtensional), and those that bend to the left or more west-trending are contractional (tranpressional). The San Clemente fault zone includes a 60-km-long restraining bend that exhibits prominent seafloor uplift in the 1300-m-deep Descanso Plain offshore of northwest Baja California, Mexico (Figs 3–4; Legg 1985; Legg & Kennedy 1991; Goldfinger *et al.* 2000). The average strike in the bend region is 308°, about 12° oblique to the left, resulting in a zone of convergent right-slip. The fault (PDZ) appears to curve gently to the left into the restraining bend at the southeast end, but terminates and steps to the right at the NW end of the bend.

The San Andreas Fault accommodates only about 50% of the total right-lateral plate boundary slip expected in the Salton Trough region (about 25 m/ka; Keller *et al.* 1982; Weldon & Sieh 1985; Harden & Matti 1989). The remaining slip must be accommodated on other faults within the 200-km-wide plate boundary in the California/Mexico border region. Peninsular Ranges faults, such as the San Jacinto and Elsinore, accommodate about 12 and 5 m/ka of right-slip (WGCEP 1995), leaving as much as 10 to 20% of the predicted relative plate motion available for faults west of the coastline. At present, the rate of right-slip on the San Clemente Fault is uncertain. Offset Quaternary seafloor morphology including submarine fan and channel features (Legg 1985; Legg *et al.* 1989; this paper), and GPS geodesy (Larson 1993; Bennett *et al.* 1997) suggest that between 1 and 10 m/ka of right-slip occurs on offshore faults.

The total Neogene and younger displacement along the San Clemente fault zone is also unknown. Movement on the San Clemente fault zone is inferred to accommodate major right-lateral components of Neogene transtension (Atwater 1970; Legg 1991; Lonsdale 1991; Crouch & Suppe 1993; Bohannon & Geist 1998). Values exceeding the 40 km originally suggested by Shepard & Emery (1941), from juxtaposing San Clemente Island alongside Fortymile Bank, have been proposed (Goldfinger *et al.* 2000). The rim of an inferred Middle Miocene crater (caldera?) appears to be offset at least 60 km in a dextral sense (Legg *et al.* 2004*b*). Deformation associated with the restraining bend may provide quantitative limits on Late Cenozoic right-slip across the San Clemente fault zone, as well as providing better understanding of restraining bend structure and evolution.

Bend morphology and fault geometry

Transpression in the bend region creates a broad asymmetrical anticlinorium, with the greatest uplift located on the northeast flank of the principal displacement zone (PDZ, Figs 3–4). Even though uplift is asymmetrical in cross-section, basin sediments are raised on both sides of the San Clemente Fault PDZ. This contrasts with fold-and-thrust belts, where crust in the footwall is downwarped and thrust beneath the hanging-wall block. Rather than being concentrated at the point of greatest fault-trace curvature (e.g. Fig. 1; Crowell 1974), the area of greatest uplift is located near the centre of the transpressional fault segment.

The broad seafloor uplift comprises two major segments separated by a saddle (Figs 3–4). Local peaks and narrow troughs exist along the fault in each pop-up. Of the two major uplifts, the northern is more symmetrical, about 6 km wide, with steep slopes, of 10 to 30°, on both the SW and northeast flanks, although steeper slopes exist where the PDZ curves around the SW flank. A narrow (1.5 km), steep-sided ridge on the SW edge of the northern uplift probably represents a fault sliver squeezed upward and offset along the PDZ. A series of youthful anticlines, with axes subparallel to the uplift and fault trend, folds the sediments and seafloor at a 1 km wavelength between the NW uplift and the Navy Channel. The southern uplift is broad and asymmetrical about 17 km wide, with the SW flank bordered by steep slopes inferred to be fault scarps, and the NE flank appearing as a more gentle, $<5°$, bedding-parallel dip-slope (Figs 6–7). Two elongate peaks centred on the southern uplift are separated by a saddle and are offset en échelon to the right. The southeastern end of the uplift consists of a low, elongate ridge, locally cut by an axial trough aligned along the PDZ (Fig. 6, line B-25).

The major active traces (PDZ) of the San Clemente Fault appear as NW-trending seafloor scarps and narrow linear valleys or troughs, generally located along the southwest flank of the major uplifts. These scarps change vergence, from NE to SW along strike, including uphill-facing scarps in some locations (Figs 3–4), typical of strike-slip faults. Two closed depressions, about 4 km long by 1 km wide, and a third smaller depression, lie at stepovers along the major fault traces. Bordered by right-stepping en echelon faults, these are interpreted as stepover (pull-apart) basins formed along the right-slip fault zone. At the NW end of the bend region, the main fault curves and steps to the right around the NW uplift, and then cuts straight

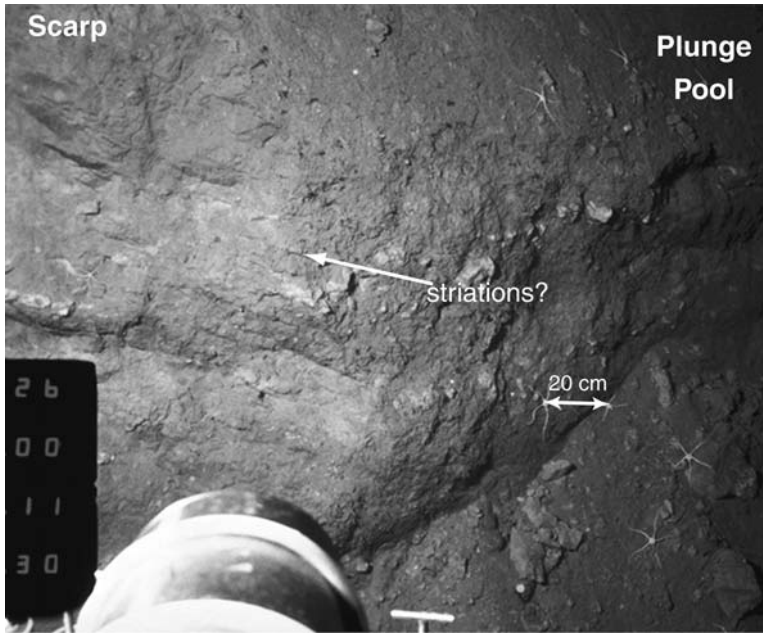

Fig. 10. Photograph from the DSV Alvin of fault scarp along the San Clemente Fault crossing the Navy fan (location in Figs 4 & 16). Subhorizontal lineations may be slickensides consistent with strike-slip. The plunge pool is cut into a scarp by deep-water (*c*. 1800 m) turbidity currents overflowing the scarp from the Navy fan. The scarp is composed of mud and layers of shells associated with ancient benthic communities at former cold seeps. Photo by C. Goldfinger (2000).

across the Navy Fan, forming a prominent scarp, 30 to 100 m high and 7 km long. This scarp is split by a semicircular embayment, about 0.5 km wide, that is inferred to be a plunge pool associated with turbidity currents on the Navy Fan (Fig. 10). Another 4 km to the northwest, this scarp dies out and the gentle slope of the Navy Fan merges into San Clemente Basin. Despite the local trace irregularities, the PDZ cuts a relatively straight 308° path across the bend region, typical of a vertical strike-slip fault. Seismic profiles confirm the vertical dip of the PDZ (Figs 6–8).

Several branch and secondary fault scarps appear to curve away from and trend parallel to the mostly linear fault scarps of the PDZ. A large, 8-km-long, north-trending east-facing set of scarps curves away from the main fault zone for 5 to 10 km at the SE end of the major uplift (Fig. 4, graben). Similar north-trending branch faults exist near the ends of the peak uplift areas (Fig. 3). The broader complex fault pattern is interpreted to represent the surface expression of a flower structure (palm-tree structure), commonly observed in cross-section along strike-slip faults (Wilcox *et al.* 1973; Harding 1985; Sylvester 1988; McClay & Bonora 2000). The systematic location and pattern of the major branch faults at the ends of peak uplift areas suggests that pre-existing structure controls the uplift geometry.

A prominent submarine channel, Descanso Fan Valley, bounds the 5-km-wide shelf along the SW flank of the southern uplift (Figs 3–4 & 7). Descanso Fan Valley, about 0.5 to 1.2 km wide, has broad meanders and uplifted relict terraces or abandoned levées along its northeast flank. Growth of the restraining bend uplift has forced the channel farther to the SW, leaving the older channel terraces and levées behind Fig. 4). The thalweg of the main channel is upwarped about 20 to 30 m where it passes the flank of the NW uplift. Hemipelagic sediments drape across the channel, conforming to the ancient seafloor channel morphology (PEL, Fig. 7, SMCS-04). Thus, tectonic upwarping continued after active channel erosion or aggradation occurred, probably during a Late Pleistocene lowstand or interglacial transgression when turbidite deposition was more frequent in the area (Dunbar 1981).

The broad, gently dipping uplift and shelf between Descanso Fan Valley and the PDZ are cut by NNW-trending fault scarps. Steep fault dips, 70 to 90°, combined with normal separation

observed in the MCS profiles (Fig. 7, SMCS-04) suggest that these are oblique-normal faults. The faults prominent near a 'knee' in the uplift SW of the PDZ are controlled by deeper acoustic basement structure that appears to be bent and forced upward due to transpression. Thus, shallow sub-seafloor oblique-extension exists directly above a basement transpressional hinge. The north trend of these scarps is consistent with west-directed extension in a NW-trending zone of dextral shear, but more likely represents the stretching of the strata above the basement pop-up. A similar NNW-trending zone of faulting on the north side of the southern uplift forms a seafloor graben, although multichannel seismic data show that the most prominent of these faults is a high-angle oblique(?) reverse fault (Fig. 7, SMCS-04, shot 4250). A deeper acoustic basement antiform also lies beneath this graben, and may correlate with the acoustic basement hinge on the southwest flank, but offset to the northwest by about 16 km of right-slip. Oblique rifting of the Inner Borderland during the Neogene evolution of the PAC–NOAM transform fault boundary could have created this north-trending structural fabric that controls the younger faulting.

Deformation history

Turbidite sedimentary sequences from nearby submarine fans (Figs 3–7) record the Late Cenozoic history of transpressional uplift along the San Clemente Fault in the bend region. Shallow sequences on the NE flank form a growth wedge with progressive northward tilting and thickening away from the PDZ (Units PEL and QT, Figs 6–7 & 11, Profile B-13). These divergent sequences lap on to or pinch out against deeper sequences and result from continued Late Quaternary uplift. Deeper sequences below Horizons 'A', 'B' and QT (Figs 6–7 & 11, Profile B-13) have relatively uniform thickness and tilt, implying pre-uplift deposition on a relatively flat-lying basin floor. Late Quaternary sedimentation rates derived from piston cores in the area (4P and 6P, Fig. 11; Dunbar 1981; Legg 1985; Lyle *et al.* 1997; Janik 2001) are used to estimate the maximum age of the deepest growth wedge, about 1.0–1.5 Ma. Sequence PEL is estimated to be about 460 $\pm$ 240 ka (Smith & Normark 1976; Legg 1985). Using the maximum observed structural relief, 700 m observed on line B-13 (Figs 4 & 11), the minimum uplift rate is estimated as 0.47 to 0.70 m/ka. The lateral slip rate is likely to be much greater for this predominantly strike-slip fault. Considering that the sedimentation rate for the turbidites below sequence PEL probably exceeds the hemipelagic rate, the initiation of uplift may be significantly younger and the uplift rate faster than these preliminary estimates.

Sedimentary sequences on the SW flank are relatively parallel with uniform thickness, with little or no onlap of deeper sequences (Figs 6–7). A shallow basin, 85 m deep, lies perched beneath the hemipelagic sequence PEL, and is inferred to have formed in the vicinity of a modern pull-apart basin between the peak uplift along the PDZ and the zone of oblique faulting to the SW above the basement hinge (Figs 3 & 7). Tilting of these basin sediments and asymmetry of the pop-up may show that this SW shelf area entered the high-relief section of the bend region at about the beginning of PEL deposition, i.e. *c*. 0.5 Ma. This could represent the time when the basement at the hinge moved into the local restraining bend at the SE side of the largest and highest peak in the bend region, about 7 km to the SE of its current position. Alternatively, tilting began when the hinge entered the local bend 14 km farther SE near the second seafloor peak. In this scenario, the initial uplift began at the farther SE peak, with the basin forming in the releasing bend saddle between the two peaks, followed by tilting and uplift when entering the second local restraining bend. At present, it is uncertain whether this buried basin is an older pull-apart, like the ones evident in the seafloor morphology.

Profiles of uplift measured relative to the flat-lying sequences away from the fault are plotted (Fig. 11, Profile B-13) to show uplift history. Relative uplift increases toward the fault, and with depth and age from the seafloor to horizon C on the northeast flank. Uplift below the shelf on the southwest flank is more uniform across the shelf, with some increase adjacent to the fault and variable increases with depth in the section. Dextral tectonic transport (advection) of the deeper and older turbidites into the bend region from the SE accounts for their uniform thickness and tilt, whereas later sequences like PEL are predominantly hemipelagic and drape over the folded and uplifted seafloor. The structural relief and inferred uplift rate on the SW side of the fault are about one-half that to the NE (Fig. 11), resulting in the asymmetry of the anticlinorium.

Santa Catalina Island

The Catalina Fault forms an 80-km-long restraining double bend (cf. Crowell 1974) between the Santa Cruz–Catalina Ridge and San Diego Trough fault zones (Figs 2 & 12). Uplift due to oblique convergence along this transpressional fault has produced Santa Catalina Island and the wide submerged shelf and slope surrounding the island. Like the San Clemente Fault bend region, the uplift is greatest

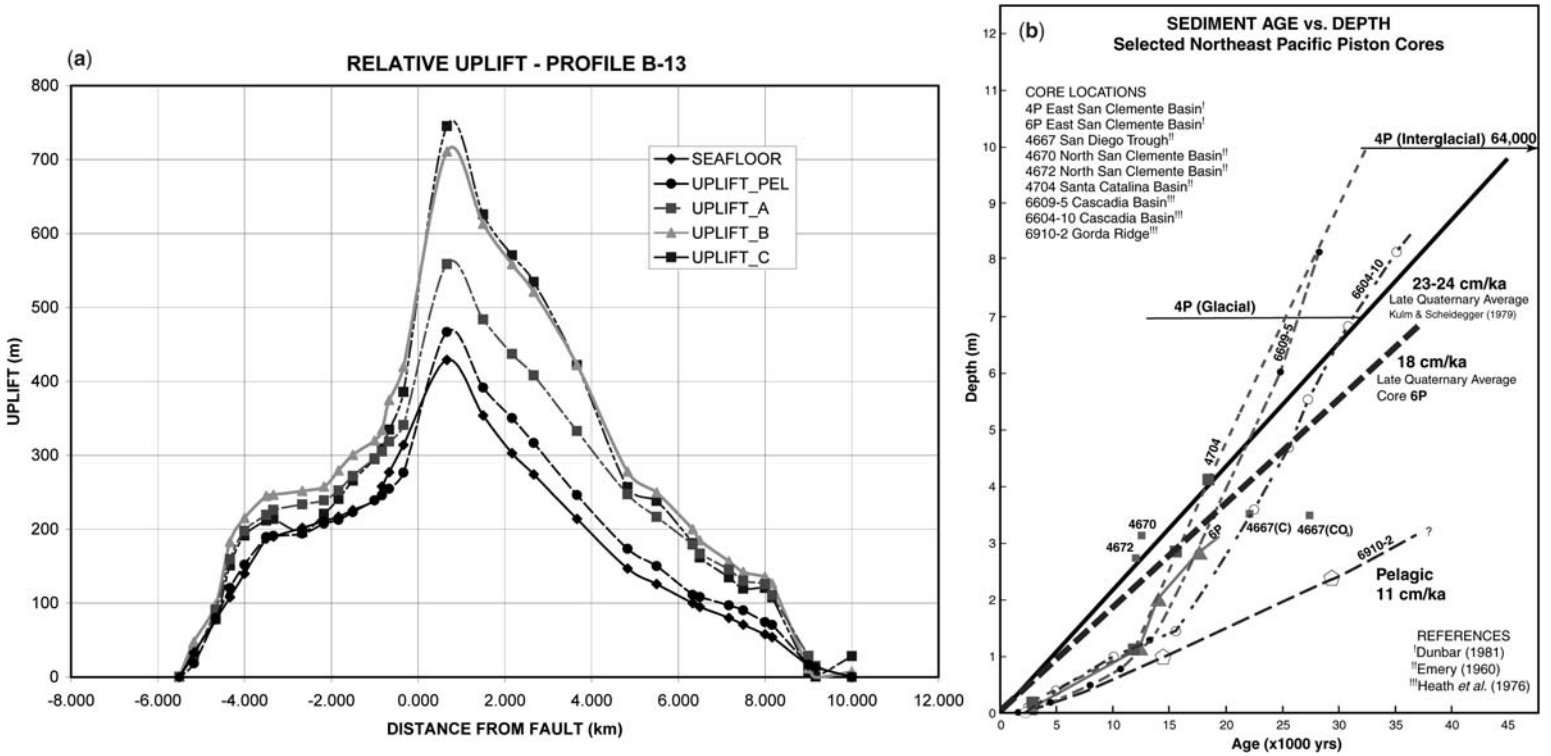

Fig. 11. (**a**) Chart showing relative uplift for sedimentary sequence horizons on profile B-13 (see Fig. 3 for profile location). Relative uplift for horizons B and C is roughly the same, implying that uplift in the bend region initiated sometime after deposition of horizon B. (**b**) Chart showing sediment age v. depth in selected piston cores from southern California and Pacific Northwest deep-water continental margins. Average sedimentation rates for turbidites in the San Clemente Basin provide estimates of age for sequence PEL. Piston cores 4P and 6P were obtained near the Navy Fan, where seismic-reflection profiles across core locations provide sediment thickness estimates. The pelagic sedimentation rate can be used for age estimates of hemipelagic drape in elevated areas where the seafloor is relatively isolated from turbidite deposition. This slow rate (0.1 m/ka) also provides a minimum rate useful for estimating the maximum age of the sedimentary sequences after compaction corrections are applied.

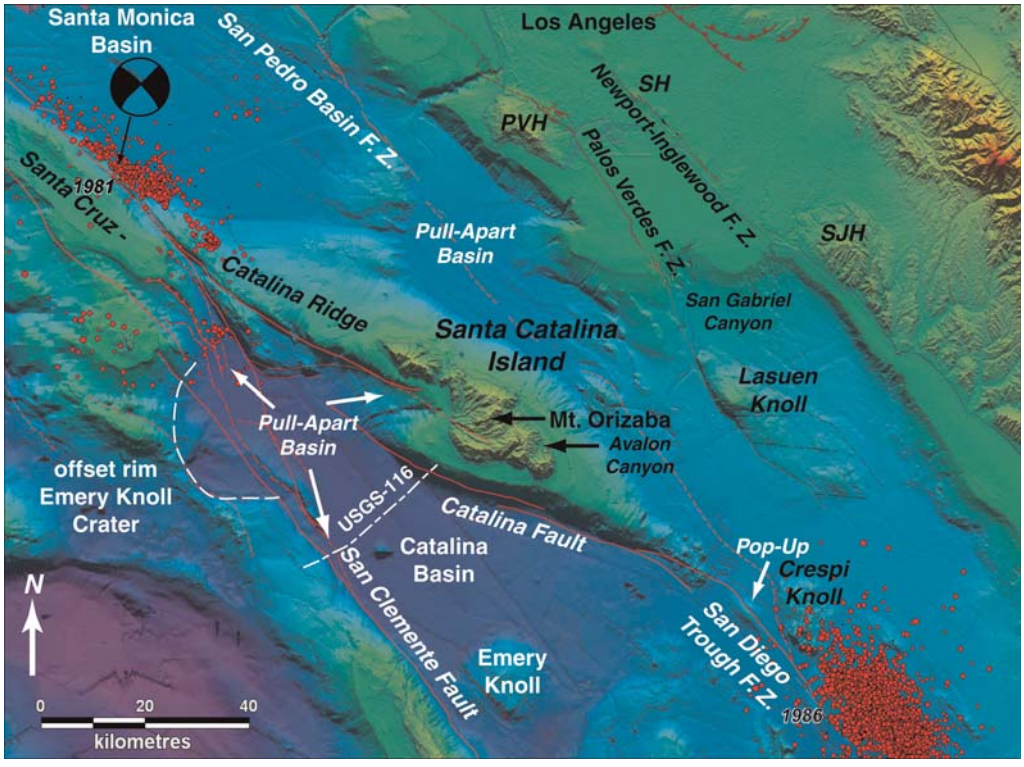

Fig. 12. Shaded relief map of Santa Catalina Island and vicinity, where several restraining-bend pop-ups and releasing-bend basins exist along major fault zones. Epicentres for two moderate earthquakes (1981 Santa Barbara Island, *M* 6.0; 1986 Oceanside, *M* 5.8) and aftershocks bound the Santa Catalina Island restraining bend (locations by Astiz & Shearer 2000; focal mechanism from Corbett 1984). Other restraining-bend pop-ups include the Palos Verdes Hills (PVH) and Lasuen knoll along the Palos Verdes fault zone, and Signal Hill (SH) and possibly the San Joaquin Hills (SJH) along the Newport–Inglewood fault zone. Small pop-ups and pull-apart basins in the vicinity of Crespi knoll are shown in Figure 14. Total relief across the Catalina Fault is almost 2000 m, from Catalina Basin to Mt Orizaba. From 60 to 72 km of right-slip on San Clemente Fault is inferred from offset of Emery Knoll crater rim (Legg *et al.* 2004*b*).

near the middle of the transpressional fault segment. The principal displacement zone (PDZ) lies along the steep escarpment on the SW flank of the uplift. To the NW, the Catalina Fault merges with the San Clemente Fault along the Santa Cruz–Catalina Ridge.

The Catalina restraining bend is comparable in scale and geometry to that of the San Bernardino Mountains segment of the San Andreas Fault in the region of the Big Bend where the San Andreas cuts across the southern California Transverse Ranges (Fig. 2). Indeed, the broad-scale geometry of the San Clemente fault system offshore of southern California is remarkably similar to that of the southern San Andreas Fault, from the Cajon Pass to the Salton Sea. Such geometric similarity may result from important similarities in the processes that create these major fault bend structures along the PAC–NOAM transform-fault plate boundary.

Bend morphology and fault geometry

Santa Catalina Island and its broad submerged platform resemble the classic 'rhomboid' pop-up structures observed in analogue models of restraining stepovers (McClay & Bonora 2001). Widespread outcrops of Catalina Schist metamorphic rocks and Miocene volcanic and plutonic rocks on the island show that the Santa Catalina pop-up involves geological basement, which produces a relatively narrow (20 km maximum width) and steep-sided morphology. Like the San Clemente Fault bend region, local irregularities in the PDZ along the Catalina Fault result in distinct secondary structures. A large, 8- to 9-km releasing (right) stepover along the NW one-third of the island creates a pronounced jog in the escarpment and sharp narrowing of the island uplift (Fig. 12). This stepover has almost 25 km of fault overlap, and major SW-trending stream

channels on Santa Catalina Island are deflected to the right by the zone of dextral shear that continues to the NW as the Catalina Ridge Fault. Although a physiographic basin is not apparent, the jog in the Catalina Escarpment is considered to represent an elevated pull-apart basin formed in this releasing fault stepover. A triangular-shaped fault-bounded crustal block at the southern end of the Santa Cruz–Catalina Ridge fits nicely into the gap created by this jog, after removing up to 17 km of right-slip on the Catalina Ridge Fault.

The NE flank of the Catalina pop-up is less steep ($<10^\circ$) than the Catalina Escarpment (almost 20°). The relatively flat floor of Catalina basin to the SW lies at depths of 1000 to 1300 m, whereas the Santa Monica and San Pedro basins are about 800 to 900 m deep. Thus, the pop-up creates a tectonic dam that traps turbidite sediments to the NW, leaving Catalina basin relatively sediment-starved (cf. Gorsline & Emery 1959). Only minor faults are mapped along the NE flank of the Catalina pop-up (Vedder *et al.* 1986).

Deformation history

Based on high-resolution multi-channel seismic profiles along the Catalina Ridge, the principal traces of the San Clemente and Santa Catalina faults have vertical to subvertical dip. Uplift predicted by a seven-segment elastic dislocation fault model of the Santa Catalina Island pop-up, matches the island/platform morphology using fault depths reaching 16 km. In the model, fault dips range from 60 to 70° for the WNW-trending oblique-slip segments beneath the island, and 80 to 90° for the NW-trending right-slip segments along Catalina Ridge and in the San Diego Trough (Legg *et al.* 2004*a*). Tomographic models of wide-angle seismic-reflection data are consistent with high-angle faulting along the SW flank of Santa Catalina Island cutting through the upper crust (ten Brink *et al.* 2000).

Catalina basin is relatively flat-floored, with sediments covering a highly irregular bedrock surface (Vedder *et al.* 1974). Shallow sedimentary sequences adjacent to the base of the Catalina Escarpment appear to thicken near the major fault stepover (Fig. 13). These sequences are elevated and probably represent a slope apron deposit from the north end of the island (Teng 1985). Distal turbidite sediments from the San Gabriel submarine canyon create a low-relief, gently SW-sloping sequence at the SE end of the basin. Sedimentary sequences elsewhere in the basin along the Catalina Escarpment are relatively uniform in thickness and uplifted. Locally thick sequences exist along the SW flank of the Catalina basin, where right stepovers along the San Clemente Fault create pull-apart basins. Deeper basin-fills with triangular cross-sections adjacent to the Catalina Fault appear to be associated with ancient pull-apart basins formed during the Neogene transtensional rifting of the Inner Borderland rather than the post-Miocene transpression at the restraining bend. Like the San Clemente Fault bend region, Late Quaternary uplift is evident on both sides of the Catalina Fault. Convergence results in crustal thickening at a subvertical oblique-slip fault, without

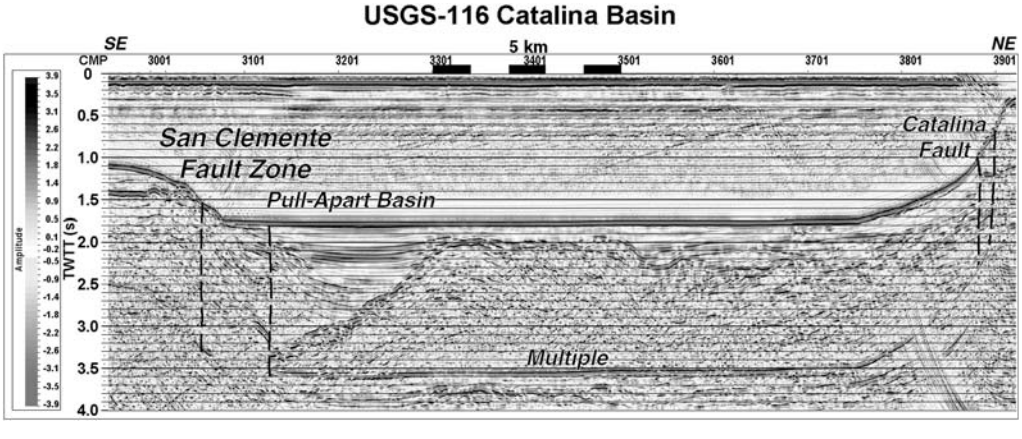

Fig. 13. Seismic-reflection profile USGS-116 across the Catalina basin (see Fig. 12 for profile location). Note the thin sediment cover over an irregular basement surface. A pull-apart basin exists where the San Clemente Fault steps to the NE to eventually merge with the Catalina Fault. The major faults have subvertical dips, typical of strike-slip faults. Convergence across the Catalina Fault has elevated Santa Catalina Island, and uplift occurs on both sides of the PDZ. Seismic data from USGS (J. Childs 2005, pers. comm.) FK migration at 4800 fps velocity was applied to 22-fold USGS stacked data.

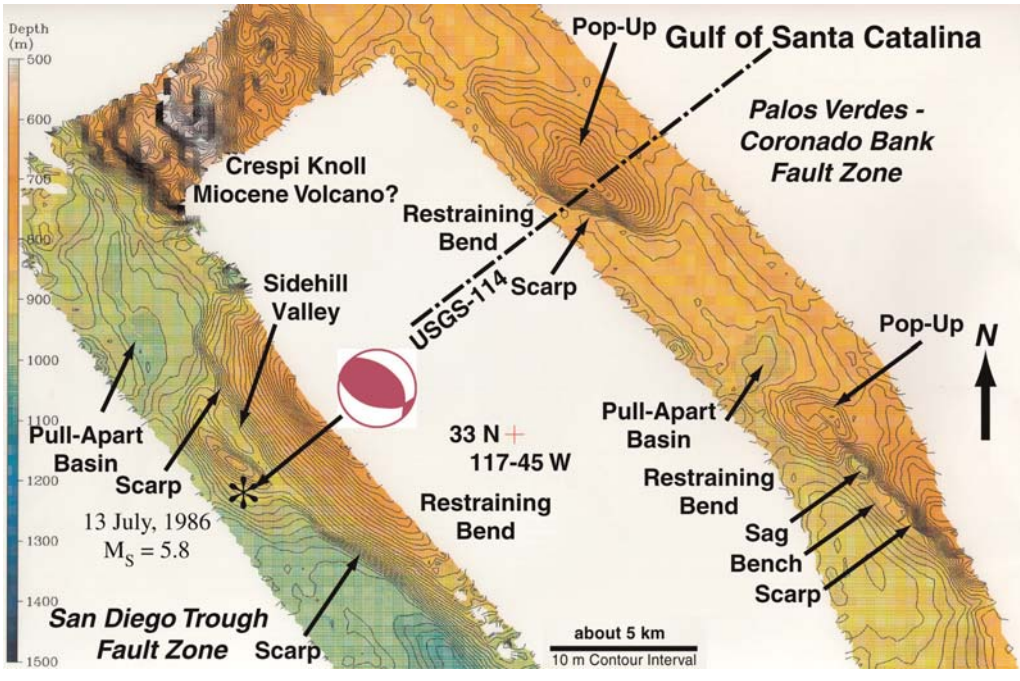

Fig. 14. SeaBeam swath bathymetry over restraining bend pop-ups and releasing stepover pull-apart basins in the northern San Diego Trough area (see Fig. 2 for map location). The southern California offshore area has many paired sets of restraining bends and releasing stepovers along the major NW-trending right-slip fault zones. The 1986 Oceanside earthquake exhibited oblique-reverse movement on a fault plane parallel to the restraining bend in the San Diego Trough fault zone (Hauksson & Jones 1988). Aftershocks spanned the region between the San Diego Trough and Coronado Bank fault zones, and included some events with strike-slip focal mechanisms.

underthrusting or basin subsidence at a reverse or thrust fault.

The lack of prominent uplifted marine terraces is noteworthy for Santa Catalina Island (Davis 2004) creating controversy regarding its uplift history. Well-defined submerged marine terraces are apparent in the bathymetry (Fig. 12; Emery 1958), whereas the uplift of sediments around the base of the escarpment surrounding the island and elevated fluvial terraces along Avalon canyon (Davis 2004) suggest Late Cenozoic uplift. Lower bathyal to abyssal microfossils from latest Miocene to Early Pliocene tuffaceous sandstone and siltstone exposed on the island (Vedder *et al.* 1979), imply that as much as 2 km of post-Miocene uplift has occurred. The topographic relief across the Catalina Fault measures about 1950 m, from Catalina basin to Mt Orizaba; upon adding another 300 m of sedimentary fill in the basin, structural relief exceeds 2200 m. Unfortunately, GPS and other geodetic data are inadequate at present to verify uplift or subsidence in recent history.

Seismicity along the Catalina Fault is minor, with a few small events (magnitude *c*. 3) recorded during the past 73 years of seismograph operation (Figs 2 & 12). More abundant activity is mapped to the NE in the San Pedro basin. Moderate earthquakes (*M* 5.8 to 6.0) ruptured at each end of the Catalina Fault bend during the 1980s (Corbett 1984; Hauksson & Jones 1988). The mainshocks and their abundant aftershock sequences may signify that the intervening transpressional fault segment is locked and accumulating strain for future large earthquakes ($M > 7$) if rupture involves most of the intervening fault segment (Legg *et al.* 2004*a*).

Other Inner Borderland restraining bends

Regionally, the California Continental Borderland abounds with restraining and releasing bend structures along the several major right-slip faults (Fig. 2). Two prominent restraining bend pop-up structures along the Palos Verdes Fault in the southern California coastal area include Lasuen Knoll and the Palos Verdes Hills (Fig. 12, Borrero *et al.* 2004; Ward & Valensise 1994). A

transtensional zone, inferred to be a releasing bend trough along the Palos Verdes Fault, separates these two large pop-ups and controls the location of the San Gabriel submarine canyon. Two smaller transpressional uplifts are found farther south along the Palos Verdes–Coronado Bank fault zone (Fig. 14). The northern feature has the classic rhomboid pop-up morphology observed in analogue models (McClay & Bonora 2001), whereas the southern feature appears as a small 1-km-wide bump at the end of an elongate ridge. Small closed depressions that probably represent local stepover basins (sags) occur along the ridge south of the pop-up, and a larger 2-km-wide stepover basin (pull-apart) is inferred to separate the two restraining bend pop-ups. The principal displacement zone (PDZ) lies along the SW flank of the uplift for the southern three of these restraining bends, and is delineated by a seafloor scarp. The Palos Verdes Hills Fault follows the NE flank of the pop-up at the SW edge of the Los Angeles basin. A steep, subvertical fault bounds the SW flank of the small rhomboidal pop-up with a sediment-filled half-graben-shaped basin to the SW, and uplifted Pliocene and older sedimentary rocks to the NE (Fig. 15). A vertical PDZ exists along the Palos Verdes Fault under San Pedro Bay, according to exploration industry seismic interpretations (Wright 1991).

Some restraining bend pop-ups appear as more symmetrical double humps in cross-section (Fig. 6, line B-25) and as pecan-shaped double bumps on the seafloor, like the feature west of Crespi knoll, between the SE end of the Catalina Fault bend and the 1986 Oceanside earthquake sequence (Fig. 12). A pull-apart basin is located south of Crespi knoll (Fig. 14) where the San Pedro Basin fault zone splits from the San Diego Trough Fault. Miocene volcanic rocks dredged from Crespi knoll, adjacent to this pull-apart, may

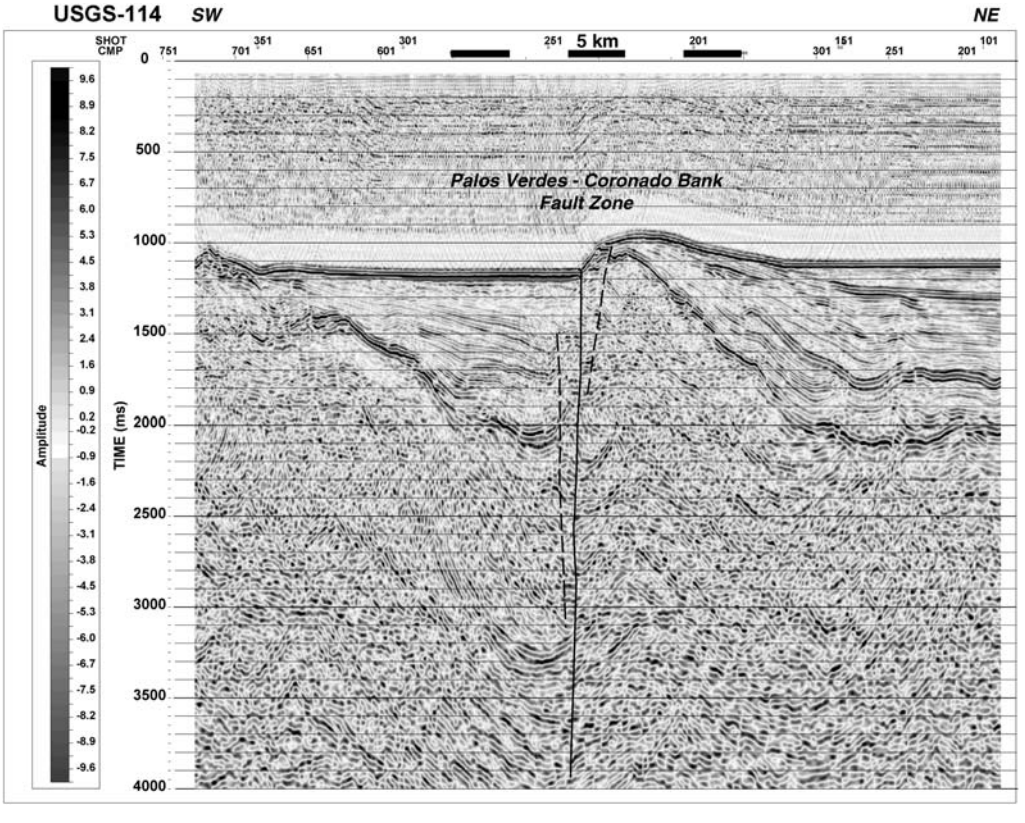

Fig. 15. Migrated 44-channel seismic-reflection profile USGS-114 across the Palos Verdes–Coronado Bank fault zone in the Gulf of Santa Catalina (see Fig. 14 for profile location; processing by C. Sorlien 1992). A small restraining-bend pop-up is juxtaposed against a small half-graben basin. Onlap of sedimentary sequences against tilted strata in both the basin and the NE flank of the uplift records contemporaneous pop-up growth and basin subsidence. Seafloor outcrops sampled on the uplift scarp from DSV Alvin were of Pliocene age (Kennedy *et al.* 1985).

indicate reactivation of an ancient extensional structure formed during the Mid-Miocene oblique rifting of the Inner Borderland. For these pop-up configurations, a near-vertical PDZ bisects the uplift, and strata dip away from the PDZ on both sides; uplift occurs on both sides of the PDZ. It is proposed that strike-slip has juxtaposed two formerly asymmetrical pop-up features to form the local double bump, as these small features are observed at the ends of larger restraining bend uplifts. Alternatively, uplift across a subvertical fault is eroded along the axial PDZ where material is weaker than on the uplift flanks, or these features are narrow crestal grabens where extension occurs above the peak transpressional uplift.

The San Diego Trough Fault has at least two other small restraining bends south of the large Catalina Fault double bend. A NW-trending ridge along the west edge of Coronado Fan Valley, at the base of the Coronado Escarpment, has been interpreted as a natural levée, although seismic reflection profiles show a rock core within this ridge (Shepard & Dill 1966). High-resolution swath bathymetry shows that relatively straight seafloor scarps along the San Diego Trough Fault are offset to the left, so that we interpret this ridge as a restraining stepover pop-up structure (Fig. 16). Uplift along the fault has forced the upper Coronado Fan Valley to turn south for about 20 km along the base of the Coronado Escarpment. The northern 14 km meanders between the inferred pop-up and the escarpment; the southern 6 km is very straight – possibly controlled by a north-trending releasing segment of the San Diego Trough Fault.

Another 22 km south along the San Diego Trough Fault, and directly east of the northern bend region of the San Clemente Fault, is a small 2.3-km-wide by 3.8-km-long seafloor pop-up (Figs 2 & 17). This pop-up exists at a single bend involving a 12° change in fault strike. Locally, there is a small $<2°$ change in fault strike, and a

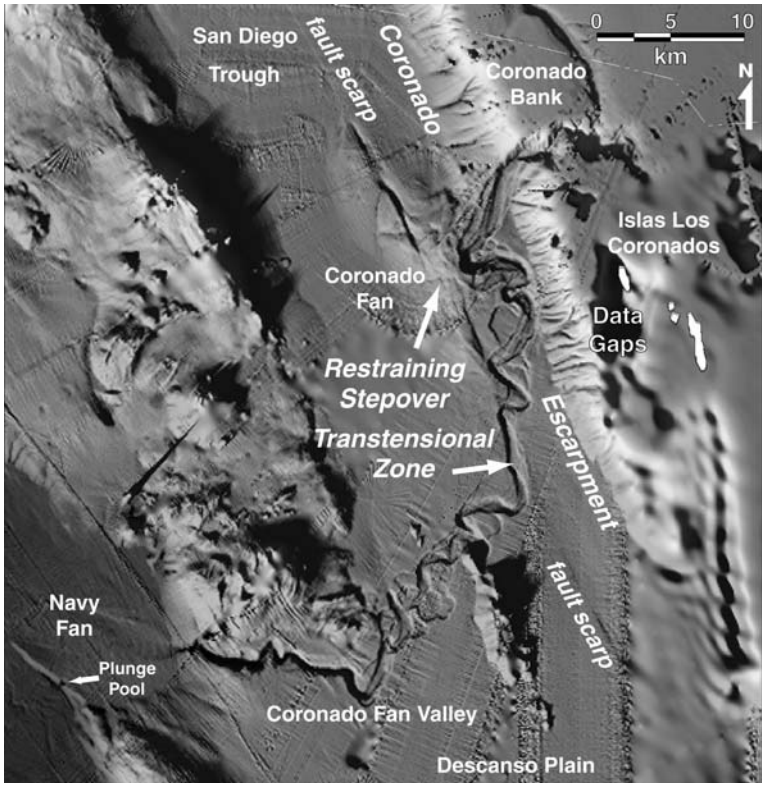

Fig. 16. Shaded relief image of Coronado canyon and the fan valley area (see Fig. 2 for map location). The San Diego Trough Fault is evident as the linear seafloor scarp cutting across the eastern side of the San Diego Trough. A left stepover in the fault zone creates an uplift that confines the Coronado Fan Valley to the east below the Coronado Escarpment. A NNW-trending fault segment forms a transtensional zone that directs the channel to the south of the restraining stepover.

500 m right (releasing) stepover from the SW to NE fault segments. Also, the SE fault appears to branch into a west-trending (281°) scarp that bounds the south edge of the pop-up structure. The high-resolution multi-channel seismic profile shows about 700 m of structural relief on this pop-up (Fig. 7, SMCS-04), although only about 70 m extends above the turbidite fill as seafloor relief. In the broader view, the SE fault segment curves gently into the area of the pop-up, from a strike of 329° to a strike of about 319°, then steps to the right about 500 m to the NW fault segment with a strike of 317°. The west-trending branch that forms the seafloor scarp results from contraction at the termination of the SE fault segment. Thus, the pop-up structure results from the combination of the change in fault trend, i.e. restraining bend, plus the termination of the SE fault segment. A similar combination may be responsible for uplift of Lasuen knoll (Fig. 12), but more detailed subsurface mapping is required to resolve that larger structure and its deformation history.

Review of the Borderland restraining-bend structure

A broad sampling of restraining bend pop-up structures, and associated releasing bend or stepover pull-apart basins, exist in the California Continental Borderland, where more than 20 Ma of evolution of the dextral Pacific–North America transform fault system has been sustained. Some of the restraining bend structures resemble those observed in analogue models, exhibiting the classic rhomboid shape, but others have distinct differences. In particular, there is an overall right-stepping en echelon pattern to the faulting, which is contrary to the typical left-stepping pattern observed in the analogue wrench fault experiments for right-slip faulting. For example, along the San Clemente

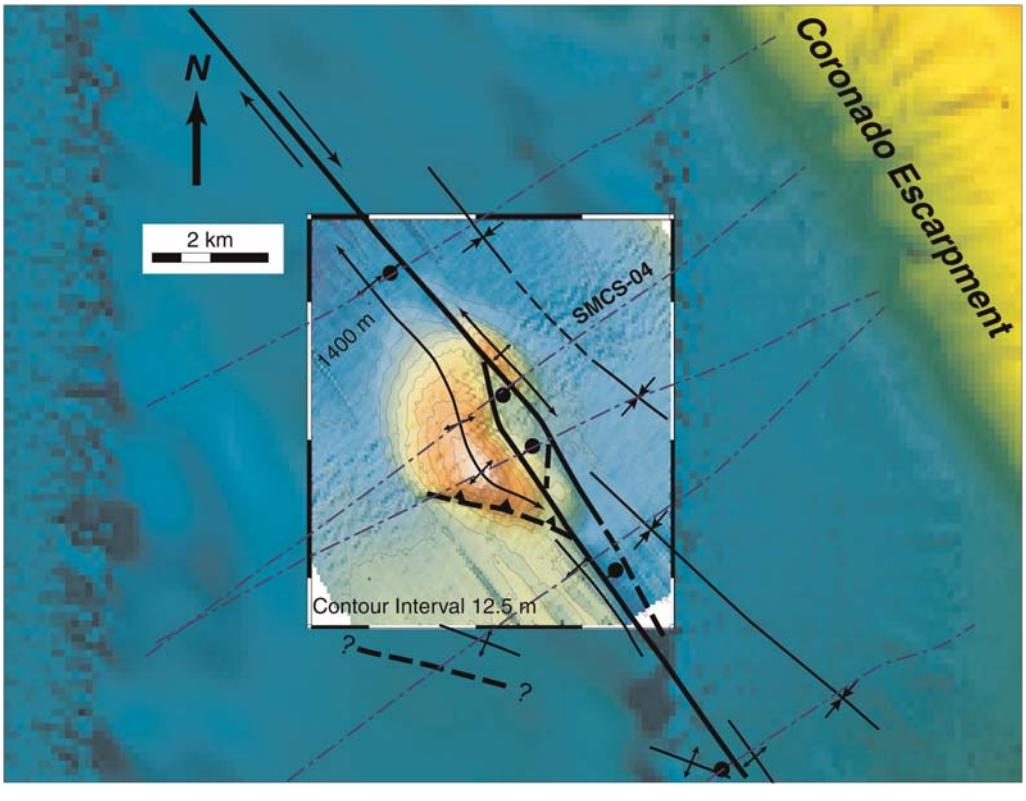

Fig. 17. High-resolution bathymetry and structural interpretation of small restraining-bend pop-up along the San Diego Trough Fault (see Fig. 2 for map location). Well-defined faults are solid with bar and ball placed on the downthrown side where seafloor is offset. Dashed faults are buried or inferred, and are queried where uncertain. Dash–dot lines mark the location of seismic profiles used to map buried faults and folds. Line SMCS-04 is shown in Figure 7. Note that a local releasing fault stepover (right en échelon offset) exists within the restraining bend (left bend).

fault zone, major fault segments step to the right in the vicinity of Navy Fan (Fig. 3), near Fortymile Bank (Fig. 2), and west of Santa Catalina Island (Figs 2 & 12). Similarly, the Catalina Fault exhibits a major right stepover along the SW side of Santa Catalina Island (Fig. 12). This right-stepping pattern resembles that of the Gulf of California, and is considered to be related to the oblique-rifting of the Inner Borderland during the Neogene time (Legg & Kamerling 2004). Two large restraining double bends display major uplift concentrated along the oblique transpressional fault segment – not at the bend where fault curvature is maximal. In contrast, a small restraining bend with releasing stepover on the San Diego Trough Fault exhibits local uplift related to a combination of fault segment termination and to the minor change in fault strike. Many transpressional pop-up structures are manifest as double bumps straddling the principal displacement zone (PDZ) of the major fault. Where soft sediments are involved, uplift exists over a broad area, with gentle seafloor slopes away from the PDZ. Where more rigid bedrock is involved, uplift is more narrow and steep-sided.

In all cases, the dip of the main strike-slip fault is very steep (70° to 80°) to vertical. This observation is the most diagnostic feature of strike-slip faults, even where a flower or palm-tree structure may be absent. The steep dip is manifest at the seafloor or ground surface as a very straight fault trace, even where high topographic relief is crossed. Uplift in the pop-up occurs on both sides of the PDZ, perhaps due to the subvertical fault dip. Typically, this uplift is asymmetrical as shortening becomes greater to one side of the PDZ. Subsidence of the footwall, common to reverse faults, is uncommon in Borderland strike-slip restraining bends.

The surface expression of flower structure appears as branching and secondary fault scarps; small pull-apart (stepover) basins; and larger-scale graben and oblique-fault branch scarps that may extend several kilometres away from the PDZ. Structural relief observed in seismic profiles across the active pop-up structures ranges from several hundred metres to more than two kilometres for Borderland restraining bends. The larger restraining bends approach 100 km lengths and are possibly locked due to enhanced normal stress in transpression between large ($M > 7$) earthquakes.

Tectonic evolution of Borderland restraining bends

Four observations common to Borderland restraining bends lead to a simple model for their tectonic evolution (Fig. 18). First, the strike of the principal displacement zone (PDZ) in the major restraining bends is parallel to the Miocene Pacific–North America (PAC–NOAM) relative motion vector(s). Catalina and Whittier faults trend about 290°, Palos Verdes Hills Fault trends about 300°, and San Clemente Fault bend region trends about 308° (Fig. 2). The clockwise rotation of these trends possibly results from the clockwise rotation of the relative plate motion vector through late Cenozoic times (Atwater & Stock 1998). Second, the major faults within the restraining bend pop-up have very steep to vertical dips. This is more consistent with formation as a strike-slip fault rather than a normal or reverse fault (Anderson 1951). Third, the pop-up structures for the major restraining bends have structurally inverted Miocene basins. Although not a sediment-filled basin, Santa Catalina Island is a volcanic centre that formed where extension thinned the crust, substantially exhuming the Catalina Schist subduction complex and providing access to upper-mantle magmatic sources (Vedder *et al.* 1979; Bohannon & Geist 1998; ten Brink *et al.* 2000). Fourth, there is an overall right-stepping en echelon character to the major right-slip fault pattern of the Borderland. Locally, this pattern persists as the pull-apart (right stepover) basin within the restraining bend pop-up. Regionally, this pattern is apparent as the major fault segments step to the right across larger pull-apart or stepover basins, as best expressed in the San Clemente fault system (Fig. 2).

Phase 1 – oblique rifting and formation of transform faults and spreading centres

The California Continental Borderland formed during the Neogene development of the PAC–NOAM transform plate boundary (Atwater 1970; Legg 1991; Lonsdale 1991; Crouch & Suppe 1993). During Mid-Miocene times, oblique rifting of the western Transverse Ranges away from the continental margin formed the Inner Borderland Rift (Legg 1991; Crouch & Suppe 1993). Pre-existing structural fabric from Mesozoic to Early Cenozoic subduction controlled the orientation of the rift, which has a trend of 330° as expressed by the San Diego Trough, roughly parallel to the modern coastline. For a displacement vector about 30° oblique to the rift trend, i.e. 290° to 308°, a complex pattern of faults forms, including mostly strike-slip faults, both dextral and sinistral, as well as extensional faults (Fig. 18, Phase 1 Withjack & Jamison 1986). New right-slip faults created to accommodate the PAC–NOAM transform motion trend NW, subparallel to the rift margins. Normal faults formed along a north–south trend.

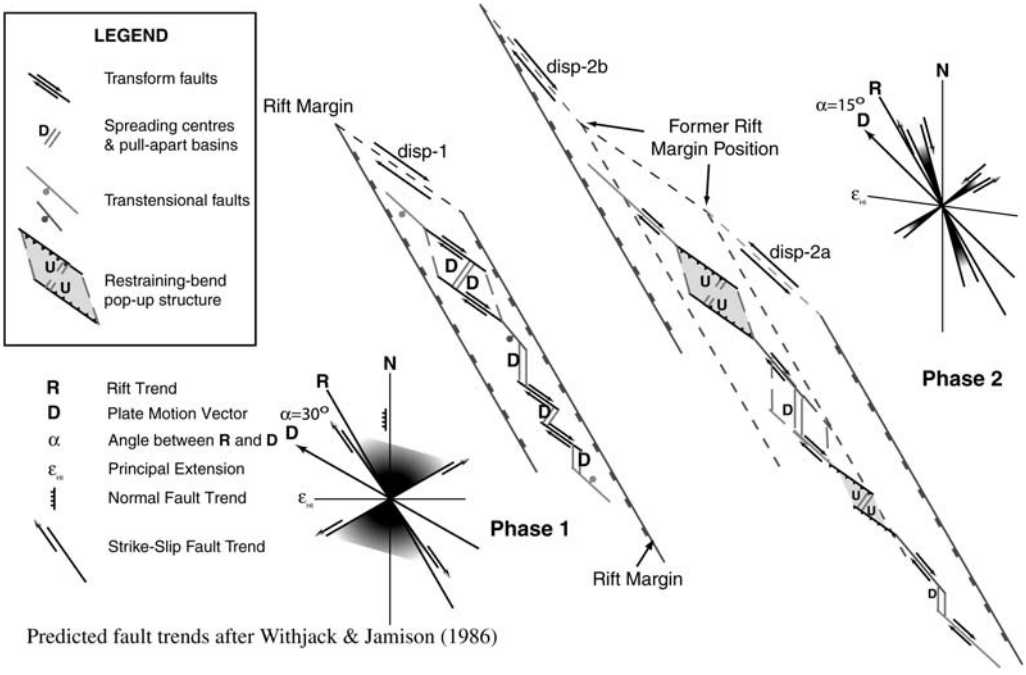

Fig. 18. Simplified model for generation of restraining bends in an evolving dextral transform plate boundary. Initial oblique rifting along transform boundary creates a series of right-stepping en echelon transform faults linked by pull-apart basins. The structural fabric from the prior tectonic boundary style (subduction for California) controls the geometry of the rift formed due to a relative motion vector more westerly than the ancient structural trend. Some new strike-slip faults will have trends oriented clockwise to the transform vector, including synthetic shears. Transtensional basins form along these faults and at the fault stepovers (pull-apart basins). Clockwise rotation of the transform plate-motion vector results in transpression along the original transform faults, and former transtensional faults may become parallel right-slip transform faults. Transtensional basins become structurally inverted and form restraining-bend pop-up structures.

However, when displacement exceeded several kilometres, most of the relative motion became concentrated on a few major right-slip faults that grew parallel to the relative plate-motion vector and linked north-trending continental rift centres. Seafloor spreading, with creation of new oceanic crust along faults orthogonal to the transform faults, did not occur, because the rift initiated in the thickened crust of a former subduction zone accretionary wedge, and extension was insufficient to create zero-thickness lithosphere.

Creation of new transform faults in the Inner Borderland Rift was facilitated by thinned continental crust that was also thermally weakened by active volcanism during Mid-Miocene times (Vedder *et al.* 1974; Weigand 1994). The transform-fault trend parallels the displacement vector, whereas synthetic Riedel shears with a more northern trend would become transtensional. Most significantly, a right-stepping en échelon pattern of right-slip transform faults linking north-trending pull-apart basins and incipient seafloor-spreading centres was created. This fault pattern resembles the modern Gulf of California transform fault system (Lonsdale 1985) and differs from the classical 'wrench fault tectonics' where dextral strike-slip results in a left-stepping en echelon pattern of synthetic Riedel shears (Wilcox *et al.* 1973; Withjack & Jamison 1986; McClay & White 1995).

Phase 2 – clockwise rotation of the relative plate-motion vector, transpression, and basin inversion

In Late Miocene times, the PAC–NOAM relative plate motion vector shifted clockwise (Fig. 18, Phase 2, Atwater & Stock 1998). Existing transform faults with the old relative motion trend, to the west or counterclockwise to the new trend, became transpressional. Other right-slip faults with trends more parallel to the new plate-motion vector became pure strike-slip, ceasing transtensional basin formation. Stepover (pull-apart) basins, previously

formed between en échelon transform faults, stopped subsiding and became structurally inverted due to transpression. With a rift trend more closely aligned with the relative plate motion vector, formation of new faults would tend to favour strike-slip on synthetic Riedel shears that could also grow into transform faults parallel to the displacement vector. Following the plate-boundary jump inland to the modern San Andreas fault system, at about 6 Ma, creation of the major southern California restraining bend (Fig. 2, 'big bend') increased the NE-directed shortening across the Inner Borderland. This latter episode is considered responsible for enhanced restraining bend pop-up formation, such as along the Palos Verdes Hills Fault and at Santa Catalina Island, and may represent a further clockwise rotation of the displacement vector (Fig. 18, Disp-2b). The Late Quaternary Pasadenan Orogeny (Wright 1991) further increased contractional strain with north-directed shortening between the western Transverse Ranges and the northern Borderland, enhancing transpressional uplift along major Borderland right-slip faults including the Santa Cruz–Catalina Ridge, Palos Verdes, and Whittier faults.

Conclusions

Borderland restraining bends exist at a wide range of scales, from a few kilometres to more than 100 km in length. Morphology of Borderland restraining-bend pop-ups is well preserved due to the low erosion rates in deep offshore basins. In plan view, Borderland pop-up morphology is generally polygonal and often rhomboidal, as observed in many analogue models. Pop-up structures involving turbidite sediments are smoother and more gently sloping than pop-ups in more rigid bedrock and basement material. The uplift is usually asymmetrical, with the principal displacement zone (PDZ) aligned along one side of the peak uplift. Unlike low-angle to moderately dipping thrust and reverse faults, where underthrusting occurs, shortening normal to the vertical strike-slip fault results in uplift on both sides of the fault. Borderland pop-ups typically involve structural inversion of ancient sedimentary basins, and extreme uplift in some large restraining bends exposes volcanic and metamorphic basement rocks. In contrast to analogue models of pop-up internal structure, the PDZ and major branch and secondary faults within the restraining bend have very steep to vertical dips. This is considered a result of evolution within an active transform fault plate boundary. An overall right-stepping en echelon fault pattern combined with the basin inversion at major restraining bends, where the PDZ trends parallel to the Miocene Pacific–North America relative plate-motion vector, suggests that Borderland restraining bends formed initially as transform faults in an oblique rift similar to the modern Gulf of California. Subsequent clockwise rotation of the relative motion vector led to creation of new transform faults parallel to the evolving plate-motion vector, and initiated transpression and basin inversion along the earlier transform faults at their pull-apart basin or incipient spreading-centre intersections.

We appreciate the careful reviews by A. Sylvester, P. Mann, M. Gordon and D. Cunningham that helped to improve this manuscript, and special thanks go to editors P. Mann and D. Cunningham for their patient support whilst completing the final manuscript. Summer intern H. Wang helped to measure the uplift at the San Clemente Fault bend region. The University of California provided support for a student cruise led by K. Macdonald to acquire new multi-beam bathymetry and high-resolution seismic data offshore of Baja California. M. Barth ensured that the seismic data were of the highest quality, and K. Broderick helped to process some of the multi-beam data. This research was supported by the Southern California Earthquake Center. SCEC is funded by NSF Cooperative Agreement EAR-0106924 and USGS Cooperative Agreement 02HQAG0008. The SCEC contribution number for this paper is 954. Support in part was also provided by USGS award numbers 01HQGR0017 (MRL) and 01HQGR0018 (CG).

References

ANDERSON, E. M. 1951. *The dynamics of Faulting*. Oliver and Boyd, Edinburgh, 206 pp.

ANDERSON, R. S. 1990. Evolution of the northern Santa Cruz Mountains by advection of crust past a San Andreas fault bend. *Science*, **249**, 397–401.

ASTIZ, L. & SHEARER, P. M. 2000. Earthquake locations in the inner Continental Borderland offshore southern California. *Seismological Society of America Bulletin*, **90**, 425–449.

ATWATER, T. 1970. Implications of plate tectonics for the Cenozoic evolution of western North America. *Geological Society of America Bulletin*, **81**, 3515–3536.

ATWATER, T. M. & STOCK, J. 1998. Pacific–North America plate tectonics of the Neogene southwestern United States – an update. *International Geologic Review*, **40**, 375–402.

AYDIN, A. & KALAFAT, D. 2002. Surface ruptures of the 17 August and 12 November 1999 Izmit and Duzce earthquakes in northwestern Anatolia, Turkey: their tectonic and kinematic significance and the associated damage. *Seismological Society of America Bulletin*, **92**, 95–106.

BENNETT, R. A., RODI, W. & REILINGER, R. E. 1996. Global Positioning System constraints on fault slip rates in southern California and northern Baja, Mexico. *Journal of Geophysical Research*, **101**, 21 943–21 960.

BIDDLE, K. T. & CHRISTIE-BLICK, N. (eds) 1985. *Strike-slip Deformation, Basin Formation, and Sedimentation.* SEPM Special Publications, **37**, 386 pp.

BILLINGS, M. P. 1972. *Structural Geology*. 3rd edn, Prentice-Hall. Englewood Cliffs, New Jersey, 606 pp.

BOHANNON, R. G. & GEIST, E. 1998. Upper crustal structure and Neogene tectonic development of the California Continental Borderland. *Geological Society of America Bulletin*, **110**, 779–800.

BOHANNON, R., EITTREIM, S. *ET AL*. 1990. A seismic-reflection study of the California Continental Borderland [abstract]. *Transactions of the American Geophysical Union*, **71**, 1631.

BORRERO, J. C., LEGG, M. R. & SYNOLAKIS, C. E. 2004. Tsunami sources in the southern California bight. *Geophysical Research Letters*, **31**, L13211.

BUTLER, R. W. H., SPENCER, S. & GRIFFITHS, H. M. 1998. The structural response to evolving plate kinematics during transpression: evolution of the Lebanese restraining bend of the Dead Sea Transform. *In*: HOLDSWORTH, R. E., STRACHAN, R. A. & DEWEY, J. F. (eds) *Continental Transpressional and Transtensional Tectonics*, Geological Society, London, Special Publications, **135**, 81–106.

CORBETT, E. J. 1984. *Seismicity and crustal structure studies of southern California: tectonic implications from improved earthquake locations*. PhD thesis California Institute of Technology, Pasadena, California, 231 pp.

CROUCH, J. K. & SUPPE, J. 1993. Late Cenozoic tectonic evolution of the Los Angeles basin and inner California borderland: a model for core complex-like crustal extension. *Geological Society of America Bulletin*, **105**, 1415–1434.

CROWELL, J. C. 1974. Origin of late Cenozoic basins in southern California. *In*: DICKINSON, W. R. (ed.) *Tectonics and Sedimentation*. SEPM Special Publications, **22**, 190–204.

DAVIS, P. 2004. The marine terrace enigma of Catalina Island – an uplifting experience? *In*: LEGG, M., DAVIS, P. & GATH, E. (eds) *Geology and Tectonics of Santa Catalina Island and the California Continental Borderland*, South Coast Geological Society Field Trip Guidebooks, **32**, Santa Ana, California, 115–121.

DEMETS, C., GORDON, R. G., ARGUS, D. F. & STEIN, S. 1990. Current plate motions. *Geophysical Journal International*, **101**, 425–478.

DEWEY, J. F., HOLDSWORTH, R. E. & STRACHAN, R. A. 1998. Transpression and transtension zones. *In*: HOLDSWORTH, R. E., STRACHAN, R. A. & DEWEY, J. F. (eds) *Continental Transpressional and Transtensional Tectonics*. Geological Society, London, Special Publications, **135**, 1–14.

DUNBAR, R. B. 1981. *Sedimentation and the history of upwelling and climate in high fertility areas of the northeastern Pacific Ocean*. PhD thesis San Diego, Scripps Institution of Oceanography.

EMERY, K. O. 1958. Shallow submerged marine terraces of southern California. *Geological Society of America Bulletin*, **69**, 39–60.

EMERY, K. O. 1960. *The Sea off Southern California, a Modern Habitat of Petroleum*. John Wiley, New York, 366 pp.

FRANCIS, R. D., SIGURDSON, D. R., LEGG, M. R., GRANNELL, R. B. & AMBOS, E. L. 1999. Student participation in an offshore seismic reflection study of the Palos Verdes fault, California Continental Borderland. *Journal of Geo-Science Education*, **47**, 22–30.

GOLDFINGER, C., LEGG, M. & TORRES, M. 2000. New mapping and submersible observations of recent activity of the San Clemente fault [abstract]. *EOS, Transactions of the American Geophysical Union*, Fall Meeting, San Francisco, **81**, 1068.

GORSLINE, D. S. & EMERY, K. O. 1959. Turbidity current deposits in San Pedro and Santa Monica Basins off southern California. *Geological Society of America Bulletin*, **70**, 279–290.

HARDEN, J. W. & MATTI, J. C. 1989. Holocene and late Pleistocene slip rates on the San Andreas fault in Yucaipa, California, using displaced alluvial-fan deposits and soil chronology. *Geological Society of America Bulletin*, **101**, 1107–1117.

HARDING, T. P. 1973. Newport–Inglewood trend, California – an example of wrench style deformation. *AAPG Bulletin*, **57**, 97–116.

HARDING, T. P. 1974. Petroleum traps associated with wrench faults. *AAPG Bulletin*, **58**, 1290–1304.

HARDING, T. P. 1985. Seismic characteristics and identification of negative flower structures, positive flower structures, and positive structural inversion. *AAPG Bulletin*, **69**, 585–600.

HARLAND, W. B. 1971. Tectonic transpression in Caledonian Spitzbergen. *Geological Magazine*, **108**, 27–42.

HARRIS, R. A., DOLAN, J. F., HARTLEB, R. & DAY, S. M. 2002. The 1999 Izmit, Turkey, earthquake: a 3D dynamic stress transfer model for intraearthquake triggering. *Seismological Society of America Bulletin*, **92**, 256–266.

HAUKSSON, E. & JONES, L. M. 1988. The July 1986 Oceanside ($M_L = 5.3$) earthquake sequence in the continental borderland, southern California. *Seismological Society of America Bulletin*, **78**, 1885–1906.

HEATH, G. R., MOORE, T. C., Jr. & DAUPHIN, J. P. 1976. Late Quaternary accumulation rates of opal, quartz, organic carbon, and calcium carbonate in the Cascadia Basin area, northeast Pacific. *Geological Society of America Memoir*, **145**, 393–409.

JANIK, A. 2001. Pleistocene sedimentation in the outer basins of the California borderlands from digitally-acquired 3.5 kHz subbottom profiles and ODP Leg 167 drilling [abstract]. *EOS, Transactions of the American Geophysical Union*, **82**, F740.

KELLER, E. A., BONKOWSKI, M. S., KORSCH, R. J. & SHLEMON, R. J. 1982. Tectonic geomorphology of the San Andreas fault zone in the southern Indio Hills, Coachella Valley, California. *Geological Society of America Bulletin*, **93**, 46–56.

KENNEDY, M. P., CLARKE, S. H., GREENE, H. G. & LONSDALE, P. F. 1985. Observations from DSRV ALVIN of Quaternary faulting on the southern California continental margin. *US Geological Survey Open-File Report*, 85–39, 26 pp.

KULM, L. D. & SCHEIDEGGER, K. F. 1979. Quaternary sedimentation on the tectonically active Oregon continental slope. *In*: DOYLE, L. J. & PILKEY, O. H. (eds) *Geology of Continental Slopes*. Society of Economic

Paleontologists & Mineralogists Special Publication, **27**, 247–263.

LANGENHEIM, V. E, JACHENS, R. C., MATTI, J. C., HAUKSSON, E., MORTON, D. M. & CHRISTENSEN, A. 2005. Geophysical evidence for wedging in the San Gorgonio Pass structural knot, southern San Andreas fault zone, southern California. *Geological Society of American Bulletin*, **117**, 1554–1572.

LARSON, K. M. 1993. Application of the Global Positioning System to crustal deformation measurements, 3, Result from the southern California borderlands. *Journal of Geophysical Research*, **98**, 21 713–21 726.

LEGG, M. R. 1985. *Geologic structure and tectonics of the inner continental borderland offshore northern Baja California, Mexico*. PhD thesis, University of California, Santa Barbara, California, 410 pp.

LEGG, M. R. 1991. Developments in understanding the tectonic evolution of the California Continental Borderland. *In*: OSBORNE, R. H. (ed.) *From Shoreline to Abyss*, SEPM Shepard Commemorative Volumes, **46**, 291–312.

LEGG, M. R. & KAMERLING, M. J. 2004. Fault trends and the evolution of the Pacific–North America transform in southern California. *EOS, Transactions of the American Geophysical Union*, Fall Meeting, San Francisco.

LEGG, M. R. & KENNEDY, M. P. 1991. Oblique divergence and convergence in the California Continental Borderland. *In*: ABBOTT, P. L. & ELLIOTT, W. J. (eds) *Environmental Perils of the San Diego Region*. San Diego Association of Geologists Guidebooks, 1–16.

LEGG, M. R., BORRERO, J. C. & SYNOLAKIS, C. E. 2004*a*. Tsunami hazards associated with the Catalina Fault in southern California. *Earthquake Spectra*, **20**, 917–950.

LEGG, M. R., LUYENDYK, B. P., MAMMERICKX, J., DE MOUSTIER, C. & TYCE, R. C. 1989. Sea Beam survey of an active strike-slip fault – the San Clemente fault in the California Continental Borderland. *Journal of Geophysical Research*, **94**, 1727–1744.

LEGG, M. R., NICHOLSON, C., GOLDFINGER, C., MILSTEIN, R. & KAMERLING, M. J. 2004*b*. Large enigmatic crater structures offshore southern California. *Geophysical Journal International*, **159**, 803–815.

LONSDALE, P. 1985. A transform continental margin rich in hydrocarbons, Gulf of California. *AAPG Bulletin*, **69**, 1160–1180.

LONSDALE, P. 1991. Structural patterns of the Pacific floor offshore of Peninsular California. *In:* DAUPHIN, P. & NESS, G. (eds) *The Gulf and Peninsular province of the Californias*. *AAPG* Memoir **47**, 87–125.

LYLE, M., KOIZUMI, I. *ET AL*. 1997. *Proceedings of the Ocean Drilling Program, Initial Reports*, **167**, ch. 5, Site 1011, 86–127.

MCCLAY, K. & BONORA, M. 2001. Analog models of restraining stepovers in strike-slip fault systems. *AAPG Bulletin*, **85**, 233–260.

MCCLAY, K. & WHITE, M. J. 1995. Analogue modelling of orthogonal and oblique rifting. *Marine and Petroleum Geology*, **12**, 137–151.

MANN, P., DRAPER, G. & BURKE, K. 1985. Neotectonics of a strike-slip restraining bend system, Jamaica. *In*: HOLDSWORTH, R. E., STRACHAN, R. A. & DEWEY, J. F. (eds) *Continental Transpressional and Transtensional Tectonics*, Geological Society, London, Special Publications, **135**, 211–226.

MINSTER, J. B. & JORDAN, T. H. 1978. Present-day plate motions. *Journal of Geophysical Research*, **83**, 5331–5334.

MOORE, D. G. 1969. *Reflection Profiling Studies of the California Continental Borderland – Structure and Quaternary Turbidite Basins*. Geological Society of America Special Papers, **107**, 142 pp.

National Ocean Survey (NOS) 1999. *Hydrographic Survey Data*. National Oceanic and Atmospheric Administration, National Geophysical Data Center, Boulder, CO.

PLAFKER, G. & GALLOWAY, J. P. 1989. Lessons Learned from the Loma Prieta, California, Earthquake of October 17, 1989. *US Geological Survey Circular*, **1045**, 48 pp.

SCHREURS, G. & COLLETTA, B. 1998. Analogue modelling of faulting in zones of continental transpression and transtension. *In*: HOLDSWORTH, R. E., STRACHAN, R. A. & DEWEY, J. F. (eds) *Continental Transpressional and Transtensional Tectonics.* Geological Society, London, Special Publications, **135**, 59–79.

SCHWARTZ, S. Y., ORANGE, D. L. & ANDERSON, R. S. 1994. Complex fault interactions in a restraining bend on the San Andreas fault, southern Santa Cruz Mountains, California. *In*: SIMPSON, R.W. (ed.) *The Loma Prieta, California, Earthquake of October 17, 1989 – Tectonic Processes and Models*. US Geological Survey Professional Papers, **1550-F**, F49–F54.

SEEBER, L. & ARMBRUSTER, J. G. 1995. The San Andreas fault system through the Transverse Ranges as illuminated by earthquakes. *Journal of Geophysical Research*, **100**, 8285–8310.

SEGALL, P. & POLLARD, D. 1980. Mechanics of discontinuous faults. *Journal of Geophysical Research*, **84**, 4337–4350.

SHEPARD, F. P. & DILL, R. F. 1966. *Submarine Canyons and Other Sea Valleys.* Rand McNally & Company, Chicago, 381 pp.

SHEPARD, F. P. & EMERY, K. O. 1941. Submarine topography of the California coast – canyons and tectonic interpretation. *Geological Society of America Special Papers* **31**, 171 pp.

SHOR, G. G., Jr, RAITT, R. W. & MCGOWAN, D. D. 1976. Seismic refraction studies in the southern California borderland, 1949–1974. *Scripps Institute of Oceanography References*, **76–13**, 70 pp.

SIEH, K. E. 1978. Slip along the San Andreas fault associated with the Great 1857 earthquake. *Seismological Society of America Bulletin*, **68**, 1421–1448.

SMITH, D. L. & NORMARK, W. R. 1976. Deformation and patterns of sedimentation, south San Clemente Basin, California borderland. *Marine Geology*, **22**, 175–188.

STONE, D. S. 1995. Structure and kinematic genesis of the Quealy wrench duplex: transpressional reactivation of the Precambrian Cheyenne belt in the Laramie basin, Wyoming. *AAPG Bulletin*, **79**, 1349–1376.

SYLVESTER, A. G. 1988. Strike-slip faults. *Geological Society of America Bulletin*, **100**, 1666–1703.

SYLVESTER, A. G. & SMITH, R. R. 1976. Tectonic transpression and basement controlled deformation in the

San Andreas fault zone, Salton Trough, California. *AAPG Bulletin*, **60**, 2081–2102.

TEN BRINK, U. S., ZHANG, J., BROCHER, T. M., OKAYA, D. A., KLITGORD, K. D. & FUIS, G. S. 2000. Geophysical evidence for the evolution of the California Inner Continental Borderland as a metamorphic core complex. *Journal of Geophysical Research*, **105**, 5835–5857.

TENG, L. S. 1985. Seismic stratigraphic study of, the California Continental Borderland basins: structure, stratigraphy, and sedimentation. PhD thesis, University of Southern California, Los Angeles, 197 pp.

TUCKER, P. M. & YORSTON, H. J. 1973. *Pitfalls in Seismic Interpretation*. Society of Exploration Geophysicists Monographs, **2**, Tulsa, OK, 50 pp.

VEDDER, J. G. 1990. Maps of California Continental Borderland showing compositions and ages of bottom samples acquired between 1968 and 1979. *US Geological Survey Miscellaneous Field Studies Map MF-2122*, three sheets, scale 1:250 000.

VEDDER, J. G., BEYER, L. A., JUNGER, A., MOORE, G. W., ROBERTS, A. E., TAYLOR, J. C. & WAGNER, H. C. 1974. Preliminary report on the geology of the Continental Borderland of southern California. *US Geological Survey*, *Miscellaneous Field Studies Map MF-624*, scale 1:500 000.

VEDDER, J. G., GREENE, H. G., CLARKE, S. H. & KENNEDY, M. P. 1986. Geologic map of the mid-southern California continental margin. California Division of Mines and Geology, *California Continental Margin Geologic Map Series*, Area 2 of 7, sheet 1 of 4, scale 1:250 000.

VEDDER, J. G., HOWELL, D. G. & FORMAN, J. A. 1979. Miocene strata and their relation to other rocks, Santa Catalina Island, California. *In*: ARMENTROUT, J. M., COLE, M. R. & TERBEST, H., JR (eds). *Cenozoic Paleogeography of the Western United States*, SEPM, Pacific Coast Paleogeography Symposium, **3**, 239–256.

WAKABAYASHI, J. 2007. Step-overs that migrate with respect to affected deposits: field characteristics and speculation on some details of their evolution. *In*: CUNNINGHAM, W. D. & MANN, P. (eds) *Tectonics of Strike-Slip Restraining and Releasing Bends*. Geological Society, London, Special Publications, **290**, 169–188.

WARD, S. N. & VALENSISE, G. 1994. The Palos Verdes terraces, California: bathtub rings from a buried reverse fault. *Journal of Geophysical Research*, **99**, 4485–4494.

WEIGAND, P. 1994. Petrology and geochemistry of Miocene volcanic rocks from Santa Catalina and San Clemente Islands, California. *In*: HALVORSON, W. L. & MAENDER, G. J. (eds) *The Fourth California Islands Symposium: Update on the Status of Resources*, Santa Barbara Museum of Natural History, Santa Barbara, CA, 267–280.

WELDON, R. J., II & SIEH, K.E. 1985. Holocene rate of slip and tentative recurrence interval for large earthquakes on the San Andreas fault, Cajon Pass, southern California. *Geological Society of America Bulletin*, **96**, 793–812.

WGCEP, Working Group on California Earthquake Probabilities. 1995. Seismic hazards in southern California: probable earthquakes, 1994 to 2024. *Seismological Society of America Bulletin*, **85**, 379–439.

WILCOX, R. E., HARDING, T. P. & SEELEY, D. R. 1973. Basic wrench tectonics. *AAPG Bulletin*, **57**, 74–96.

WITHJACK, M. O. & JAMISON, W. R. 1986. Deformation produced by oblique rifting. *Tectonophysics*, **126**, 99–124.

WOODRING, W. P., BRAMLETTE, M. N. & KEW, W. S. W. 1946. Geology and paleontology of the Palos Verdes Hills, California. *US Geological Survey Professional Paper*, **207**, 145 pp.

WRIGHT, T. L. 1991. Structural geology and tectonic evolution of the Los Angeles basin. *In*: BIDDLE, K. T. (ed.) *Active Margin Basins. AAPG* Memoirs, **52**, 13–134.